Biochemical Pharmacology 195 (2022) 114864

Contents lists available at ScienceDirect

Biochemical Pharmacology

journal homepage: www.elsevier.com/locate/biochempharm

# Dictamnine, a novel c-Met inhibitor, suppresses the proliferation of lung cancer cells by downregulating the PI3K/AKT/mTOR and MAPK signaling pathways☆

Jiaojiao Yu [a,1], Lijing Zhang [a,1], Jun Peng [c,d], Richard Ward [e], Peiqi Hao [a], Jiwei Wang [a], Na Zhang [a], Yang Yang [a], Xiaoxi Guo [a], Cheng Xiang [a], Su An [a,b,*], Tian-Rui Xu [a,b,*]

[a] Faculty of Life Science and Technology, Kunming University of Science and Technology, Kunming 650500, China
[b] State Key Laboratory of Primate Biomedical Research, Kunming University of Science and Technology, Kunming 650500, China
[c] Department of Thoracic Surgery, the First People's Hospital of Yunnan Province, Kunming 650032, China
[d] The Affiliated Hospital of Kunming University of Science and Technology, Kunming 650032, China
[e] Centre for Translational Pharmacology, Institute of Molecular Cell and Systems Biology, College of Medical, Veterinary and Life Sciences, University of Glasgow, Glasgow G12 8QQ, UK

ARTICLE INFO

*Keywords:*
Dictamnine
c-Met
Lung adenocarcinoma
PI3K/AKT/mTOR
MAPK
Gefitinib resistance

ABSTRACT

Dictamnine (Dic), a naturally occurring small-molecule furoquinoline alkaloid isolated from the root bark of Dictamnus dasycarpus Turcz., is reported to display anticancer properties. However, little is known about the direct target proteins and anticancer mechanisms of Dic. In the current study, Dic was found to suppress the growth of lung cancer cells in vitro and in vivo, and to attenuate the activation of PI3K/AKT/mTOR and mitogen-activated protein kinase (MAPK) signaling pathways by inhibiting the phosphorylation and activation of receptor tyrosine kinase c-Met. Moreover, the binding of Dic to c-Met was confirmed by using cellular thermal shift assay (CETSA) and drug affinity responsive target stability (DARTS) assay. Among all cancer cell lines tested, Dic inhibited the proliferation of c-Met-dependent EBC-1 cells with the greatest potency ($IC_{50}$ = 2.811 μM). Notably, Dic was shown to synergistically improve the chemo-sensitivity of epidermal growth factor receptor-tyrosine kinase inhibitor (EGFR-TKI)-resistant lung cancer cells to gefitinib and osimertinib. These results suggest that Dic is a c-Met inhibitor that can serve as a potential therapeutic agent in the treatment of lung cancer, especially against EGFR TKI-resistant and c-Met-dependent lung cancer.

## 1. Introduction

Among all cancer types, lung cancer is still the leading cause of cancer-related deaths around the world and more than 85% of all lung cancer cases are classified as non-small-cell lung cancer (NSCLC). Improved understanding of the molecular mechanisms that cause tumor progression and metastasis of lung cancer has revolutionized the treatment of NSCLC. An oncogenic driver mutation has been identified in two-thirds of NSCLC patients. The tumorigenesis and malignant progression are usually caused by the hyper-activation of the two key signaling cascades, the PI3K/AKT/mTOR pathway and the Ras-Raf-MEK-ERK (also called the mitogen-activated protein kinase (MAPK)) pathway. The most common activating oncogenic mutations or fusions identified in lung cancer patients are receptor tyrosine kinase EGFR, serine/threonine-protein kinase K-Ras and B-Raf mutations, anaplastic lymphoma kinase (ALK) and proto-oncogene receptor tyrosine kinase

*Abbreviations:* CCK8, Cell Counting Kit-8; CETSA, cellular thermal shift assay; DARTS, drug affinity responsive target stability; Dic, Dictamnine; EdU, 5-ethynyl-2′-deoxyuridine; EGFR-TKI, epidermal growth factor receptor-tyrosine kinase inhibitor; EMT, epithelial-mesenchymal transition; FAK, focal adhesion kinase; GSK-3β, glycogen synthase kinase 3β; HGF, hepatocyte growth factor; MAPK, mitogen-activated protein kinase; MMP-2, matrix metalloproteinase-2; MMP-9, matrix metalloproteinase-9; mTOR, mammalian target of rapamycin; NSCLC, non-small-cell lung cancer; RTK, receptor tyrosine kinase; STAT3, signal transducer and activator of transcription 3.

☆ Category: Antibiotics and Chemotherapeutics.

* Corresponding authors at: Faculty of Life Science and Technology, Kunming University of Science and Technology, Kunming 650500, China.
*E-mail addresses:* aslxj@mail.ustc.edu.cn (S. An), tianruixu@kust.edu.cn (T.-R. Xu).

[1] These authors contributed equally to this work.

https://doi.org/10.1016/j.bcp.2021.114864
Received 5 October 2021; Received in revised form 20 November 2021; Accepted 26 November 2021
Available online 30 November 2021

(ROS1) fusions, which lead to the aberrant activation of PI3K/AKT/mTOR and MAPK pathways. The identification of these candidate oncogenic driver mutations in NSCLC and the findings of increasing number of clinically available inhibitors directly targeting these driver mutations provide a great opportunity to improve prognosis in patients with NSCLC. However, nearly all patients will develop resistance to targeted therapies due to intrinsic or acquired resistance [1,2].

Previous studies have reported that higher expression of c-Met is observed in 61% of NSCLCs and correlates with poor prognosis in NSCLC patients. c-Met is a receptor tyrosine kinase with only a single known ligand, the hepatocyte growth factor (HGF). Binding of HGF to c-Met stimulates c-Met receptor activation and then triggers downstream signaling pathways including PI3K/AKT/mTOR and MAPK pathways. Abnormal c-Met signaling can be activated by the somatic mutation or amplification of *MET*, or the overexpression of the c-Met receptor which drivers tumorigenesis and is related to metastasis and poor prognosis in a wide range of major human cancers including NSCLC. Indeed, it is well known that aberrant c-Met activity can confer lung cancer with acquired resistance to EGFR-TKI [3]. Although some c-Met-targeted agents including crizotinib, cabozantinib and tepotinib have been approved by the U.S. Food and Drug Administration (FDA) for the treatment of locally advanced or metastatic NSCLC patients (crizotinib and tepotinib) and patients with advanced renal cell carcinoma or hepatocellular carcinoma (cabozantinib), obstacles such as potency, selectivity, safety, and specificity have been encountered [4].

Dictamnine (4-methoxyfuro[2,3-b]quinolone, Dic), is a major bioactive component isolated from the root bark of Dictamnus dasycarpus Turcz. (Rutaceae). Dic, as a bioactive natural furoquinoline alkaloids, has been reported to possess many beneficial pharmacological activities, such as anti-platelet-aggregation, antibacterial, anti-mitosis, vascular-relaxing and anti-inflammation [5]. Because of its outstanding bio-pharmacological activities, Dic is usually used as a herbal medicine and recommended for the treatment of a variety of diseases including eczema, rheumatic arthritis, coronary atherosclerosis, jaundice hepatitis and others [5]. In addition, Dic has shown potent proliferation-inhibition and apoptosis-induced activities in various cancer-derived cell lines, such as human cervix, colon, oral carcinoma and human breast cancer cells [6]. Recently, Dic was reported to induce cell cycle arrest at low concentration and cell apoptosis at high concentration via mitochondria and caspase 3-independent mechanisms in A549 cells [7]. However, the detailed molecular mechanisms by which Dic induces apoptosis of A549 cells need to be further investigated.

In this study, we showed that Dic can suppress the activation of the two classical signaling cascades, PI3K/AKT/mTOR and MAPK pathways by directly targeting receptor tyrosine kinase c-Met, leading to the inhibition of lung cancer cell proliferation and metastasis. Additionally, Dic was shown to induce apoptosis in lung cancer cells via the intrinsic apoptosis pathway and to increase gefitinib sensitivity of EGFR-TKI-resistant PC9 cells through down-regulation of the activation of the c-Met signaling pathway.

## 2. Materials and methods

### 2.1. Patient specimens

A total of 20 paired NSCLC tissues and their adjacent non-tumor tissues were collected from patients who underwent curative surgical resection in the department of thoracic surgery, the First People's Hospital of Yunnan Province. All patients were diagnosed and confirmed by experienced pathologists, and none of the patients underwent adjuvant chemotherapy or radiation treatment prior to surgery. This study was approved by Ethics Committee of Kunming University of Science and Technology and followed the Declaration of Helsinki principles, and informed consent was obtained from all patients (protocol code KMUST2019SK012 and issued on 5/3/2019).

### 2.2. Antibodies and reagents

Dic (HPLC $\geq$ 98%) was obtained from Chengdu Herbpurify Co., Ltd. (Chengdu, China), and was prepared by dissolving the compound in ethyl alcohol and diluted in DMSO. Antibodies against pTyr1230-c-Met (ab5662), c-Met (ab39075), E-cadherin (ab40772), N-cadherin (ab18203), EGFR (ab52894), pTyr1068-EGFR (ab40815), paxillin (ab32084) and pTyr118-paxillin (ab109547) were from Abcam (Cambridge, UK). Antibodies to detect pSer17-AKT (5473), AKT (11E7), pTyr458-PI3K (4228), PI3K (4249), pTyr705-STAT3 (4113), STAT3 (12640), B-Raf (L12G7), pSer445-B-Raf (2696S), ERK (4695S), pThr202/Tyr204-ERK (9101S), Cleaved-caspase-7 (D198), IL-1β (3A6) and PARP-1 (9542) were obtained from CST (Cell Signaling Technology, Danvers, MA, USA). Antibodies against pSer2448-m-TOR (sc-293133), m-TOR (sc-517464), pSer9-GSK-3β (sc-373800), GSK-3β (53921), β-catenin (sc-7963), c-Myc (sc-40), cyclin D1 (sc-166210), pSer722-FAK (sc-374668), pTyr397-FAK (sc-81493), FAK (271195), MMP-2 (sc-13594), MMP-9 (sc-21733), β-Actin (sc-47778) were purchased from Santa Cruz Biotechnology (Santa Cruz, CA, USA). Antibody against Vimentin (V6630) was obtained from Sigma. Antibody against GAPDH (60004) was obtained from Proteintech Group, Inc. (Rosemont, USA). Antibodies against Tubulin (05–661) and Ki67 (AB9260), polyvinylidene fluoride membrane (IPVH00010) were from Millipore (Merck Millipore Ltd., County Cork, Ireland). Antibodies against CDK1 (AF0111) were purchased from Beyotime (Beyotime Biotechnology, Shanghai, China). Gefitinib, osimertinib, savolitinib and crizotinib were obtained from Topscience (Topscience Co. Ltd., Shanghai, China). Polyvinylidene fluoride membrane (IPVH00010) was from Millipore (Merck Millipore Ltd., County Cork, Ireland). Cell Counting Kit-8 (C0039), Apoptosis and Necrosis Assay Kit (C1056), TUNEL Apoptosis Assay Kit (C1090), EdU Cell Proliferation Kit (C0088S) were purchased from Beyotime (Beyotime Biotechnology, Shanghai, China). TRIzol reagent (180411) was obtained from Ambion (Thermo Fisher Scientific, Inc. Waltham, MA, USA). FastStart Essential DNA Green Master (32597600) was supplied by Roche (Roche Diagnostics, Shanghai, China). RevertAid™ First Strand cDNA Synthesis Kit (K1622) was obtained from Thermo (Thermo Scientific, Waltham, MA, USA).

### 2.3. Cell lines and cell culture

A549 (human non-small cell lung adenocarcinoma) cell line was obtained from Kunming Institute of Zoology, Chinese Academy of Sciences. Human lung carcinoma cell lines H1299, PC9 and EBC-1, liver cancer cell line HepG2, renal cell carcinoma cell line ACHN and cervical carcinoma cell line HeLa were purchased from the Cell Bank of the Chinese Academy of Sciences (Shanghai, China). Cells mentioned above were maintained in the RPMI-1640 (Hyclone, USA) supplemented with 10% (vol/vol) fetal bovine serum (FBS) (Gibco, Invitrogen) and antibiotics (10 mg/mL streptomycin sulfate, and 100 mg/mL penicillin G). To establish a gefitinib-resistant cell line, the PC9 cells were initially exposed to gefitinib at 0.2 μM for about 7 days. Then the cells were transferred to and cultured in medium without gefitinib for about 14 days. Following the above steps, the exponential growth cells were harvested and seeded in 96-well microtiter plates, the concentration of gefitinib was increased from 0.2 μM to 5 μM. After about six months, the gefitinib-resistant PC9 cells (PC9-GR) were established.

### 2.4. Bioinformatics analysis

The Gene Expression Profiling Interactive Analysis (GEPIA) browser (http://gepia.cancer-pku.cn/) is a friendly web-based tool to explore customizable functionalities based on the data provided by TCGA (https://tcga-data.nci.nih.gov/tcga/) and the Genotype-Tissue Expression project (GTEx, https://www.gtexportal.org/home/index.html). GEPIA was used to identify the transcriptional expression of c-Met between lung cancer and normal tissues. The prognostic value of c-Met

expression in lung cancer patients was analyzed by using the Kaplan-Meier plotter online database (http://kmplot.com/analysis/).

### 2.5. CCK-8 cell proliferation assay

The viability of cancer cells was determined by using the CCK-8 assay according to the manufacturer's protocol. Cancer cells were seeded in 96-well plates ($5 \times 10^3$ cells per well) and cultured for 24 h. The cells were treated with varying concentrations of Dic (0, 50, 100, 200 μM) for 2, 24, 48 and 72 h. Then 10 μL CCK-8 (Beyotime Biotechnology, Shanghai, China) was added to each well, and incubated at 37 °C for 1.5 h. The absorbance of each well was measured at a wavelength of 450 nm by using a microplate reader.

### 2.6. Combination study with gefitinib or osimertinib

PC9GR cells were treated with Dic (12.5–200 μM) and gefitinib (0.6–10 μM) or osimertinib (0.6–10 μM) alone or in combination at 1:20 (gefitinib:Dic) or 1:10 (osimertinib:Dic) fixed molar ration. After 48 h, the inhibitory effect of PC9GR cells was evaluated by CCK8 assay, the combination index (CI) was evaluated by Chou-Talalay method with CompuSyn software [8,9], and CI = (D)1/(DX)1+(D)2/(DX)2. CI > 1 indicated antagonism, CI = 1 additive effects, and CI < 1 synergy.

### 2.7. EdU cell proliferation assay

A549 cells cultivated in 96-well plates ($5 \times 10^3$ cells per well) were treated with different concentrations of Dic (0, 50, 100, 200 μM) for 24 and 48 h. After the administration of 30 μM 5-ethynyl-2′-deoxyuridine (EdU; Beyotime Biotechnology, Shanghai, China) to each well, the cells were continually incubated for 2 h at 37 °C. Then the cells were fixed with 4% paraformaldehyde in PBS for 15 min at room temperature. After the removal of the fixative, A549 cells were washed with PBS and permeabilized with 0.3% Triton X-100 for another 15 min, the cells were incubated with 100 μL 0.3% hydrogen peroxide solution for 20 min. After washing three times with 3% BSA in PBS, 50 μL Click Reaction Solution was added to each well and the cells were incubated for 30 min at room temperature. The Click Reaction Solution was discarded and the washing repeated, 20 μL Streptavidin-HRP was added and incubated for another 30 min. After washing with 3% BSA in PBS, 100 μL TMB was added to each well and incubated for about 30 min, the absorbance of each well was measured at 650 nm.

### 2.8. Apoptosis assay

In order to measure cell death and apoptosis, cells were treated with Dic (0, 50, 100, 200 μM) for 24 h and then collected for Hoechst 33342/propidium iodide (PI) staining with an apoptosis and Necrosis Assay Kit (Beyotime Biotechnology, Shanghai, China). The stained cells were observed and photographed under a confocal microscope (Nikon A1, Tokyo, Japan), and the images analyzed using the ImageJ software program (NIH, Bethesda, MD). The percentage of dead cells was then calculated according to the following: PI positive cells/total cells × 100. Cell apoptosis was also analyzed by TUNEL Apoptosis Assay Kit (Beyotime Biotechnology, Shanghai, China). Experiments were conducted according to the manufacturer's instructions. In short, after appropriate experimental treatment, cells grown in 6-well plates were washed with PBS and fixed with 4% paraformaldehyde solution for 30 min. After washing with PBS for three times, the cells were then incubated with TUNEL staining buffer containing terminal deoxynucleotidyl transferase and Cy3-labeled dUTP for 60 min. Following washing with PBS, images of cells were acquired with a fluorescence microscope (Olympus,. Melville, NY, USA).

### 2.9. Colony formation assay

For plate colony formation assays, 500 cells in the logarithmic phase were plated into 12-well plates with Dic (0, 50, 100, 200 μM) and incubated for 14 days. The cell culture medium was refreshed every three days. When the cells grew to form visible colonies, the supernatants were discarded and the colonies were fixed with 4% paraformaldehyde for 30 min, and then washed with PBS and stained with crystal violet for 15 min. For soft agar colony formation assay, PC9GR cells suspended in complete culture media were added to 0.7% agar in a top layer over a base layer of 0.8% agar. Media containing gefitinib or Dic alone or gefitinib plus Dic were added every other day for 3 weeks. Cell colonies were counted under an inverted microscope using the Image-Pro Plus software (Media Cybernetics, Inc. Rockville, MD). The assays were performed three times independently.

### 2.10. Transwell migration and matrigel invasion analysis

The migration and invasion assay were carried out using the transwell chambers (Corning Costar, Cambridge, Massachusetts, pore size 8 μm). A549 cells were treated with Dic (0, 50, 100, 200 μM) for 24 h. Cells were then trypsinized, washed, and resuspended in serum-free RPMI-1640. Migration assays and invasive assays were performed using the uncoated transwell chamber and the chamber coated with Matrigel (BD Sciences, Franklin Lakes, NJ, USA), respectively. The Matrigel was diluted with DMEM medium (3:1) and dropped onto the chamber and incubated at 37 °C for 2 h. A total of 100 μL cell suspension ($5 \times 10^5$/mL) was inoculated into the upper chamber, the bottom compartment contained 600 μL RPMI-1640 supplemented with 10% FBS to serve as a chemoattractant. After incubation for 36 h, transwell inserts were washed 3 times with PBS, fixed with 4% paraformaldehyde and stained with 0.1% crystal violet. The invading cells on the lower surface of the transwell insert were visualized with a light microscope, and counted in 5 randomly selected visual fields. The assays were performed three times independently.

### 2.11. Wound healing assay

The effects of Dic on the migratory behavior of lung cancer cells were assayed by means of a wound healing assay using a culture-insert (ibidi GmbH, Am Klopferspitz 19, Martinsried, Germany) according to the manufacturer's instructions. 200 μL cell suspension ($1.5 \times 10^5$ cells/mL) was applied to the Culture–Insert of each well and allowed to grow to a confluent monolayer at 37 °C and 5% CO2 for 24 h. The insert was gently removed using sterile tweezers, and the cells were washed twice with PBS to remove any loose cells and fresh medium containing mitomycin was added. A549 cells were treated with Dic (0, 50, 100, 200 μM) and Photographs were taken at 0, 24 and 48 h to assess cell migration into the wound using a light microscope.

### 2.12. Sphere formation assay

To investigate the effect of Dic on lung cancer stem cells, sphere formation assays were performed. Approximately $1 \times 10^4$ A549 cells were seeded into ultra-low attachment 6-well plates (Corning Inc, Corning, NY, USA) and cultured in serum-free DMEM/F-12 (1:1 ratio) media supplemented with B27 supplements (Thermo Fisher Scientific, Waltham, MA, USA), 20 ng/mL bFGF and 20 ng/mL rhEGF. Cells received treatment with various concentrations of Dic for 48 h at 72 h after cell seeding. The medium was exchanged every 3 days. After 2 weeks, cell spheres with diameters ≥ 50 μm were counted using a microscope.

### 2.13. Cell adhesion assay

A549 cells were treated with Dic (0, 50, 100, 200 μM) for 24 h and

were then seeded into 96-well plates pre-coated with 10 μg/mL fibrinogen, 10 μg/mL collagen type IV, and cultured at 37 °C for 30 min. Wells coated with 100 μg/mL poly-L-lysine were employed as a control condition. Subsequently, the medium was discarded, and the non-adherent cells were carefully removed by washing the cells three times with PBS. The attached cells were fixed with 4% paraformaldehyde for 30 min and stained with 0.1% crystal violet for 20 min at room temperature. Excess crystal violet was washed away using PBS and 100 μL of acetic acid was added to each well with gentle shaking for 10 min to dissolve the purple crystals. Absorbance was measured at 590 nm by a Microplate Reader. The quantified cellular adhesion results were normalized to control cells and were represented as relative absorbance.

### 2.14. Quantitative real-time PCR analysis

Total RNA was extracted from cells using TRIzol regent. The RNA (5 μg) was then reverse transcribed into cDNA using Revert Aid First Strand cDNA Synthesis Kit (Thermo Fisher Scientific, Waltham, MA, USA) according to the manufacturer's protocol. The level of mRNA was measured by real-time PCR using FastStart Essential DNA Green Master Mix (Roche Diagnostics, Shanghai, China) and was normalized to GAPDH. The sequences of primers used in the experiment were listed in Table 1. The reaction was performed using the LightCycler® 96. The results of q-PCR were expressed relative to threshold cycle (CT) values and fold changes were calculated using the $2^{-\Delta\Delta CT}$ method.

### 2.15. Western blot analysis

Western blotting was used to analyze the protein levels. Cells were collected and lysed with RIPA buffer. The nuclear protein and cytoplasmic Protein were extracted using the Nuclear and Cytoplasmic Protein Extraction Kit (Beyotime Biotechnology, Shanghai, China). Proteins of cell lysates were quantified by Enhanced BCA Protein Assay Kit (Beyotime Biotechnology, Shanghai, China). Equal amounts of cell lysate were separated on an SDS-PAGE gel and transferred to the PVDF membrane. After being blocked with 5% non-fat milk, the membranes were probed with primary antibodies overnight at 4 °C. The primary antibodies were as follows: anti-c-Met, anti-phospho-c-Met, anti-PI3K, anti-phospho-PI3K, anti-AKT, anti-phospho-AKT, anti-m-TOR, anti-phospho-m-TOR, anti-STAT3, anti-phospho-STAT3, anti-B-Raf, anti-phospho-B-Raf, anti-ERK, anti-phospho-ERK, anti-GSK-3β, anti-phospho-GSK-3β, anti-β-catenin, anti-c-Myc, anti-cyclin D1, anti-CDK1, anti-IL-1β, anti-GAPDH, anti-Actin, anti-Tubulin, anti-H2A. After subsequent washing with TBST, the membranes were then incubated with corresponding secondary antibodies for 1.5 h at room temperature. Protein bands were visualized by a chemiluminescence system (GeneGnome, Syngene, UK).

### 2.16. Cellular thermal shift assay (CETSA)

CETSA was performed using cell lysates and intact cells as previously described [10,11]. For a CETSA in A549 cell lysates, A549 cells were lysed with lysis buffer (50 mM Tris-HCl pH 7.2, 150 mM NaCl, 1.5 mM $MgCl_2$, 0.2% NP-40, 5% glycerol, 25 mM NaF and 1 mM $Na_3VO_4$) supplemented with 0.1% protease inhibitor cocktail. The cell suspensions were rapidly frozen and thawed three times using liquid nitrogen, and incubated on ice for 30 min, the lysates were centrifuged at 20000 × g for 20 min at 4 °C, supernatants were transferred to new tubes and protein concentrations were measured by BCA Protein Assay Kit. The cell lysates were diluted with appropriate volume of lysis buffer, and 50 μL of the lysates at 0.6 mg/mL were incubated with DMSO or Dic at different concentrations for 2 h at room temperature and then heated individually at different temperature for 3 min in a PCR machine (Applied Biosystems). The heated lysates were centrifuged to separate the precipitated proteins from the soluble fractions. The equal portions of the supernatants were loaded onto SDS-PAGE gels followed by Western blot analysis. For a CETSA in intact A549 cells, the cells cultured in 12-well plates ($3.0 \times 10^5$ cells/well) were treated with different concentrations of Dic for 2 h, the control cells were exposed to an equal volume of DMSO. After incubation, the cells were washed with PBS and 500 μL of lysis buffer was added to each well, then the lysates were heated and analyzed by Western blotting as described above.

### 2.17. Drug affinity responsive target stability (DARTS)

DARTS was used to assess the binding affinity of Dic to c-Met using protease protection from pronase digestion (Roche Applied Science, Inc.) as previously described [12]. A549 cells were washed with cold PBS and lysed using cold M−PER lysis buffer (Thermo Scientific, Inc.) supplemented with a protease inhibitor cocktail and phosphatase inhibitors. The cell lysates were centrifuged at 20000 × g for 10 min at 4 °C, and the supernatants were diluted with 10 × TNC buffer (500 mM Tris-HCl pH 8.0, 500 mM NaCl and 100 mM $CaCl_2$). The lysates in 1 × TNC buffer were incubated with DMSO or Dic at the indicated concentrations for 2 h at room temperature. After incubation, each sample was proteolyzed with 1 μg pronase to every 3000 or 4000 μg of total protein in lysate for 20 min at room temperature. Proteolysis was stopped by adding 5 × SDS sample loading buffer (250 mM Tris-HCl pH 6.8, 10% SDS, 50% glycerol, 0.5% bromophenol blue and 5% β-mercaptoethanol) and boiling at 100 °C for 5 min. An equal portion of each sample was loaded onto SDS-PAGE gels and analyzed by Western blotting.

### 2.18. Molecular modeling of Dic with c-Met

The crystal structure of c-Met was obtained from the Protein Data Bank (PDB: 4IWD). AutoDock Tool was utilized to prepare the input PDBQT file for c-Met and set the size and the center of the grid box. Hydrogen atoms were added and all water molecules were removed from the structure of c-Met. The center of the grid box was set with the dimension (X = -8.833, Y = 12.926, and Z = -16.482) using 0.1 nm spacing and a box size of 20 × 20 × 20. The three-dimensional structure of Dic was generated using Open Babel software. Molecular docking of

**Table 1**
Sequences of primer used in qPCR.

| Gene symbol | Sense (5′-3′) | Antisense (5′-3′) |
|---|---|---|
| c-Met | TACCCCAGCCCAAACCATTT | CCCACCACTGGCAAAGCAAA |
| Bax | GCAAACTGGTGCTCAAGGCCC | TCGCTTCAGTGACTCGGCCA |
| Bid | ACTGTTGAGTGGCTGAAT | AGTGGCGACAGAATCCGC |
| Bcl-2 | AGGCTGGGATGCCTTTGTGGAA | ACCAGGGCCAAACTGAGCAGA |
| Bcl-XL | TCCTTGTCTACGCTTTCCACG | GGTCGCATTGTGGCCTTT |
| BAG3 | CATCCAGGAGTGCTGAAAGTG | TCTGAACCTTCCTGACACCG |
| MCL-1 | CCAAGAAAGCTGCATCGAACCAT | CAGCACATTCCTGATGCCACCT |
| E-cadherin | GCTGGACCGAGAGAGTTTCC | CGACGTTAGCCTCGTTCTCA |
| N-cadherin | AGGCTTCTGGTGAAATCGCA | TGCAGTTGCTAAACTTCACATTG |
| Vimentin | TCCGCACATTCGAGCAAAGA | TGATTCAAGTCTCAGCGGGC |
| GAPDH | AAGGTCGGAGTCAACGGATTTGG | TTCTCAGCCTTGACGGTGCC |

Dic at the active site of c-Met was achieved using AutoDock Vina. The best pose on the basis of binding affinity and docking was selected and post-docking results were analyzed using LigPlot + .

### 2.19. Subcutaneous xenografts in nude mice

All animal experiments were approved by our Institutional Animal Care and Treatment Committee (protocol code KMUST2019SK027 and issued on 5/3/2019). Four to five weeks-old female BALB/c nude mice were purchased from Shanghai Lingchang Biotechnology Co., Ltd. (Shanghai, China) and maintained under specific pathogen-free conditions with controlled light and humidity, receiving food and water ad libitum. Before inoculating into mice, A549 cells were washed twice and counted, approximately $5 \times 10^6$ cells suspended in 100 μL PBS/animal were inoculated subcutaneously into the right armpits of mice. The mice were randomly assigned into 2 groups, an experimental group and a control group, each of 6 mice. Treatment with Dic began 9 days after inoculation of the cells when the tumors reached a volume of 100–150 $mm^3$. The experimental group was treated with i.p. injections of Dic (50 mg/kg body weight) for the next 15 days, while the control group received an equal volume of vehicle. All mice were weighted daily during the treatment time, and tumor volume was calculated using the following formula: $0.5 \times \text{length} \times (\text{width})^2$. One day after the last treatment mice were sacrificed, and then the tumors were dissected, weighed and subjected to hematoxylin-eosin (HE) staining combined with immunohistochemistry (IHC) analysis.

### 2.20. Hematoxylin-eosin, immunohistochemistry and fluorescence staining

Solid tumors from control and treatment groups were fixed with 4% paraformaldehyde and embed in paraffin for H&E staining and IHC. Tissue sections were deparaffinized in xylene, dehydrated in graded ethanols and finally hydrated in distilled water, the sections were then counterstained with HE. For IHC, epitope retrieval was performed by directly boiling the slides in 10 mM sodium citrate (pH 6.0) for 30 min, immunohistochemistry was performed according to the manufacturer's guidelines and recommendations. Briefly, the sections were treated with 3% hydrogen peroxide for 10 min to quench endogenous peroxidase and non-specific binding was blocked with 5% normal goat serum/TBST (Cell Signaling Technology, Cambridge, USA #5425). The slides were incubated overnight at 4 °C with anti-Ki67 antibody (rabbit polyclonal antibody, diluted 1:200, Merck-Millipore, Darmstadt, Germany #AB9260). After incubation, the tissues were incubated with Signalstain Boost IHC detection reagent (HRP, rabbit, Cell Signaling Technology, Cambridge, USA #8114) for 30 min at room temperature and detected with the Signalstain DAB substrate kit (Cell Signaling Technology, Cambridge, USA #8059), followed by counterstaining with hematoxylin. Apoptotic cells in tumors were detected using a terminal deoxynucleotidyl transferase dUTP nick-end labeling (TUNEL) assay according to the manufacturer's protocol (KeyGEN BioTECH, Nanjing, China #KGA700). Images were taken using an Olympus microscope and quantified by the image analyzer ImageJ.

### 2.21. Statistical analysis

GraphPad Prism was used for statistical analysis. All quantitative Data were presented as the mean ± standard deviation (SD). Statistically significant differences were obtained using an unpaired two-tailed student's *t*-test or by one-way ANOVA. A P value of $<0.05$ was considered statistically significant.

## 3. Results

### 3.1. Dic inhibits the proliferation of cancer cells expressing c-Met and attenuates HGF-activated proliferative response in A549 cells

Dic is a small-molecule 4-methoxyfuro (2,3-b) quinolin compound with a molecular weight of 199.21 Da (Fig. 1A). c-Met, the only known high-affinity receptor for hepatocyte growth factor (HGF), is usually overexpressed, highly activated, and sometimes mutated in NSCLC tissues [13]. Bioinformatics analysis also indicated that c-Met expression in both lung adenocarcinoma (LUAD) and lung squamous cell carcinoma (LUSC) from TCGA database was significantly higher than that in normal tissues (Fig. 1B). Survival analysis showed that patients with high c-Met expression had a poor overall survival rate (Fig. 1C). The high expression of c-Met in lung cancer tissues was further confirmed by Western blotting and qRT-PCR analysis (Fig. 1D and 1E). The clinicopathologic characteristics and c-Met expression of NSCLC patients were displayed in Table 2.To determine the specific inhibitory effect of Dic on c-Met-dependent proliferation of cancer cells, various types of cancer cells with high expression of c-Met were treated with different concentrations of Dic, and the c-Met low-expressing cell line HEK293 was used as control. As shown in Fig. 1F and G, Dic significantly inhibited the proliferation of A549 and H1299 human non-small-cell lung cancer cells, HeLa cervical cancer cells, HepG2 liver cancer cells, as well as ACHN renal carcinomal cells in a dose-dependent manner, while having no obvious effect on the proliferation of HEK293 cells (Fig. 1H). Dic also showed inhibitory effect on the proliferation of a normal lung epithelial cell line HPAEpiC at relatively higher concentrations (Fig. 1H). In addition, Dic significantly suppressed the phosphorylation levels of c-Met in H1299, HeLa, HepG2 and ACHN cells in a concentration-dependent manner. The inhibitory effect of Dic on A549 cell proliferation was further confirmed by EdU assay (Fig. 1I). Furthermore, when A549 cells were serum-starved overnight and treated with HGF (100 ng/mL) or Dic (100 μM) for 24 h, or treated with indicated concentrations of Dic for 24 h in the presence of HGF (100 ng/mL), cells stimulated with HGF alone exhibited greater proliferative response than did cells from control group, and whilst treatment with Dic resulted in a concentration-dependent inhibition of proliferative response induced by HGF in A549 cells (Fig. 1J). The molecular profile of cancer cells used in this study was listed in Table 3.

Two c-Met inhibitors, savolitinib and crizotinib, were used as a positive control, and the effect of Dic on cell proliferation compared to savolitinib and crizotinib in A549 cells was investigated. As presented in Fig. 1K, 10 μM savolitinib, 10 μM crizotinib and the indicated concentrations of Dic significantly inhibited the proliferation of A549 cells, and remarkably suppressed the phosphorylation of c-Met (Fig. 1L). Additionally, 10 μM savolitinib displayed less proliferation inhibitory activity than 10 μM crizotinib and Dic (50, 100 and 200 μM), while 10 μM crizotinib, 100 and 200 μM Dic had comparable growth inhibitory activity against A549 cells (Fig. 1K).

The effect of Dic on cell proliferation compared to savotinib and crizotinib was also observed in c-Met-dependent EBC-1 cells. Dic inhibited the proliferation of EBC-1 cells and c-Met phosphorylation in a dose-dependent manner (Fig. 1M and N). These three c-Met inhibitor displayed a comparable potency against the proliferation EBC-1 cells at the same concentration (0.1 μM), while the inhibitory effect of Dic on the proliferation of EBC-1 cells ($IC_{50} = 2.811$ μM) was weaker than that of crizotinib, but stronger than that of savotinib as the inhibitors concentration increased (Fig. 1P). Additionally, Dic (50 μM) had activity comparable to savotinib (10 μM) and crizotinib (10 μM) in inhibiting c-Met phosphorylation (Fig. 1Q). Notably, Dic even significantly inhibited the expression of c-Met in a dose-dependent manner in EBC-1 cells (Fig. 1N, O and Q).

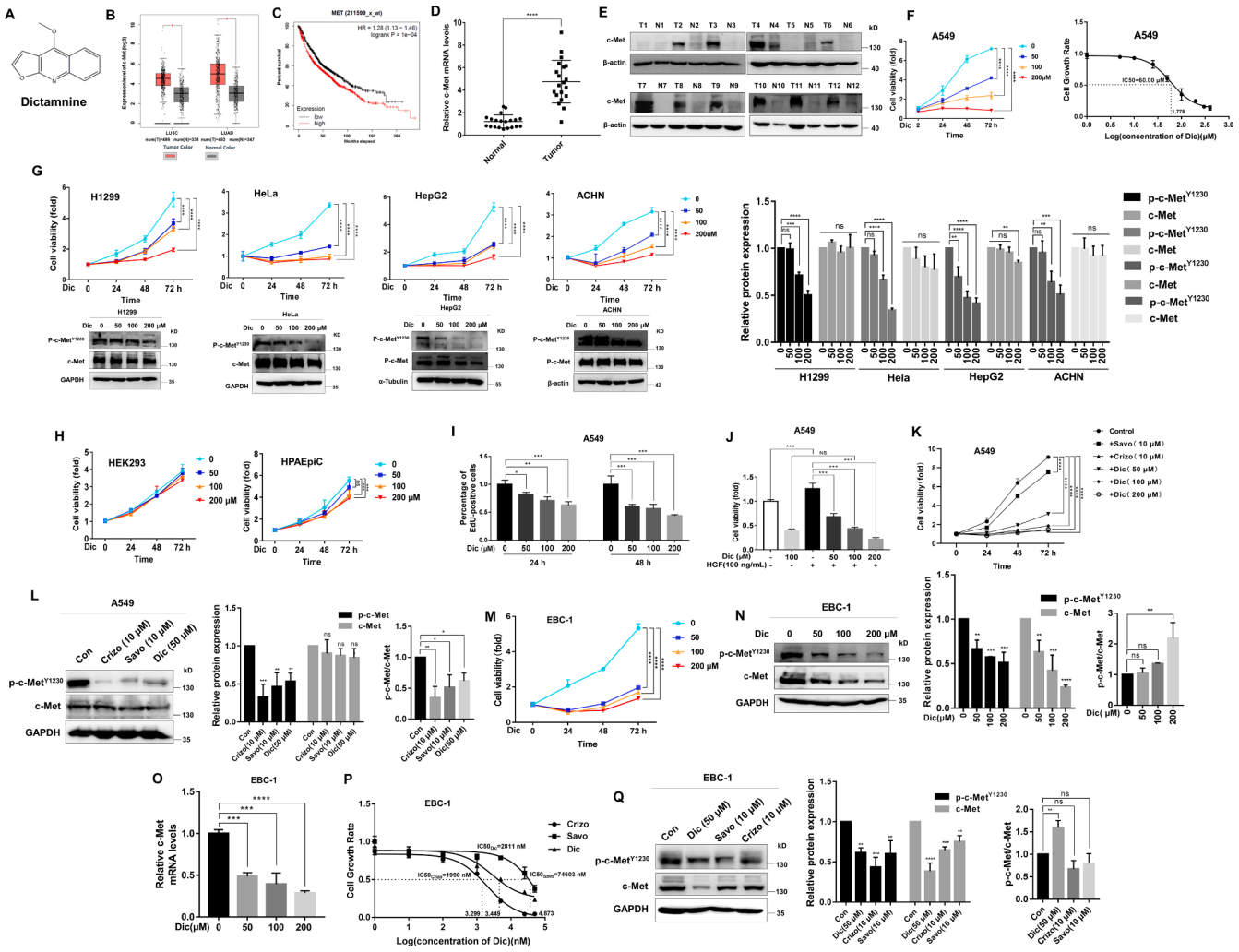


**Fig. 1. Validation of c-Met up-regulation in NSCLC clinical specimens and Dic inhibits the proliferation of cancer cells with high expression of c-Met.** (**A**) Chemical structure of Dic. (**B**) Bioinformatics analysis of c-Met mRNA expression levels in LUAD, LUSC and normal lung tissues from the TCGA dataset. (**C**) The prognostic value of c-Met was evaluated in the TCGA cohort. (**D**) Quantitative RT-PCR assay of relative c-Met mRNA expression levels in 20 pairs of human clinical NSCLC tissues (Tumor) and adjacent noncancerous tissues (Normal), ****P < 0.0001 as compared with the control (one-way ANOVA with Dunnett's test). (**E**) Western blotting assay of c-Met protein level in 12 pairs of human clinical NSCLC samples (T: tumor tissue, N: paired adjacent noncancerous tissue). Various types of cancer cells including A549 (**F**), H1299, HeLa, HepG2 and ACHN (**G**) with high expression of c-Met or c-Met low-expressing HEK293 cells and normal lung epithelial cell line HPAEpiC (**H**) used as control were treated with different concentrations of Dic for the indicated times, following which cell proliferation was analyzed using the CCK8 assay (n = 3). Western blot analyses were conducted to assess the effects of Dic on the phosphorylation of c-Met in H1299, HeLa, HepG2 and ACHN cells after treatment with different concentrations of Dic for 24 h. (**I**) EdU incorporation assays were applied to examine the EdU positive A549 cells after treatment with Dic for 24 or 48 h. (**J**) The effect of Dic on HGF-activated proliferation response in A549 cells was evaluated by CCK-8 assay. (**K**) A549 cells were treated with 10 μM savolitinib (Savo), 10 μM crizotinib (Crizo) or different concentrations of Dic for the indicated times, following which cell viability was analyzed by the CCK8 assay (n = 3). (**L**) The effect of Dic, savolitinib (Savo) or crizotinib (Crizo) on the phosphorylation of c-Met in A549 cells. Cells were treated with 10 μM crizotinib (Crizo), 10 μM savolitinib (Savo) or 50 μM Dic for 36 h and analyzed by Western blotting, DMSO (0.1%) served as negative control. (**M**) The effect of Dic on the proliferation of EBC-1 cells. Cells were treated with the indicated concentrations of Dic for 24, 48 and 72 h. CCK8 was performed to measure cell viability. (**N**) The effect of Dic on the expression and phosphorylation of c-Met in EBC-1 cells. Cells were treated with indicated concentrations of Dic for 36 h and analyzed by Western blotting, DMSO (0.1%) served as negative control. (**O**) The effect of Dic on the mRNA expression levels of c-Met was determined by qRT-PCR normalized with GAPDH. (**P**) EBC-1 cells were incubated with indicated concentrations of crizotinib (Crizo), savolitinib (Savo) or Dic for the 48 h, following which cell viability was analyzed by the CCK8 assay (n = 3). (**Q**) The effect of Dic, savolitinib (Savo) or crizotinib (Crizo) on the phosphorylation of c-Met in EBC-1 cells. Cells were treated with 50 μM Dic, 10 μM savolitinib (Savo) or 10 μM crizotinib (Crizo) for 36 h and analyzed by Western blotting, DMSO (0.1%) served as negative control. For F-K, M, O and P, data were expressed as the mean ± S.D. from three independent experiments. For L, N and Q, images presented are representative of at least three independent experiments, and data are expressed as the mean ± S.D. The significance was determined by one-way ANOVA with Dunnett's test and *P < 0.05, **P < 0.01, ***P < 0.001 and ****P < 0.0001 for the designated treatment versus the control. ns, no significant differences.

### *3.2. The synergistic anti-proliferative activity of Dic and gefitinib or osimertinib in PC9GR cells*

We successfully established a gefitinib-resistant PC9 (PC9GR) cell line from the gefitinib-sensitive PC9 cell line after approximately six months of gefitinib treatment (Fig. 2A). We also evaluated the effect of osimertinib on the proliferation inhibition of PC9GR cells. As shown in Fig. 2B, osimertinib could significantly inhibit the proliferation of parental PC9 cells at a concentration of as low as 2 nm. However, osimertinib showed no obvious effect on the proliferation of PC9GR cells even at a concentration of 2 μM. Therefore, PC9GR cells have cross-resistance to osimertinib. While PC9 and PC9GR cells were found to be sensitive to Dic, and their proliferation was inhibited in a concentration-dependent manner (Fig. 2C and D).

**Table 2**
Clinicopathologic Characteristics and c-Met expression of NSCLC patients.

| Clinic pathology | | c-Met level | |
|---|---|---|---|
| | | Low: n (%) | High: n (%) |
| Gender | Male | 2 (10.0) | 13 (65.0) |
| | Female | 0 (0) | 5 (25.0) |
| Age | <60 | 2 (10.0) | 7 (35.0) |
| | ≥60 | 0 (0) | 11 (55.0) |
| Tumor subtypes | Squamous cell carcinoma | 1 (5.0) | 6 (30.0) |
| | Adenocarcinoma | 1 (5.0) | 8 (40.0) |
| | Large cell carcinoma | 0 (0) | 4 (20.0) |
| Tumor stage | T1-T2 | 2 (10.0) | 15 (75.0) |
| | T3-T4 | 0 (0) | 3 (15.0) |
| Regional lymph nodes stage | N0 | 2 (10.0) | 13 (65.0) |
| | N1-N3 | 0 (0) | 5 (25.0) |
| Distant metastasis stage | M0 | 2 (10.0) | 16 (80.0) |
| | M1-M3 | 0 (0) | 2 (10.0) |

Gene expression values of *c-Met* were classified, compared to normal tissues, as high (>1) or low (<1). The pathological diagnoses and classifications were made according to American Joint Committee on Cancer (AJCC) cancer staging manual, 7th ed. Because the sample size is less than 40, it is inaccurate to use *p* value representing the probability from a chi-square test for c-Met levels between variable subgroups.

**Table 3**
Driver gene alterations of cancer cell lines used in this study.

| Cell lines | Driver gene alterations |
|---|---|
| A549 | *KRAS* G12S |
| H1299 | *NRAS* Q61K |
| PC9 | *EGFR* exon 19 deletion |
| PC9GR | *EGFR* exon 19 deletion and *MET* amplification |
| EBC-1 | *MET* amplification |
| HeLa | p53 inactivated and small telocentric chromosome |
| HepG2 | *NRAS* Q61K/L |
| ACHN | *NF2* gene loss |

Then the combined effects of Dic and gefitinib or osimertinib on proliferation inhibition were measured by CCK8. As shown in Fig. 2E and F, the combination of gefitinib (1 μM) or osimertinib (2 μM) and Dic (25, 50, 100 and 200 μM) achieved a synergistic effect on proliferation inhibition in PC9GR cells and resulted in significantly higher inhibition of cell growth relative to single-gefitinib or osimertinib treatment over 72 h. EdU assay showed that single-Dic treatment was as effective as the combination of Dic and gefitinib as far as proliferation inhibition of PC9GR was considered (Fig. 2G).

Next, 1:10 (gefitinib:Dic) or 1:20 (osimertinib:Dic) fixed molar ration for combination in PC9GR cells were selected. Compared with Dic and gefitinib or osimertinib alone in the 48 h inhibition rate of PC9GR cells, Dic in combination with gefitinib or osimertinib significantly increased PC9GR cells proliferation-inhibition (Fig. 2H and J). According to CCK8 data, Chou-Talalay method was used to calculate the combination index (CI) (Table 4 and Table 5). Furthermore, the effect versus CI curves shown in Fig. 2I and K exhibit a synergistic proliferation-inhibition effect (CI < 1) of Dic combined with gefitinib or osimertinib, and most of the data points are positioned below the line of additive effects.

PC9 cells are known to harbor an in-frame deletion in exon 19 of EGFR gene leading to EGFR hyperactivation , while the mutational status of EGFR in gefitinib and osimertinib double-resistant PC9GR cells is unclear, so PCR and DNA sequencing were used to analyzed EGFR mutations. In our study, no other EGFR hotspot mutations including L718V, G719A, G724S, S768I, T790M, L792H/V, G796S/C, C797S, L833V, H835V and L858R, with the exception of exon 19 deletion mutation, were detected in gefitinib and osimertinib double-resistant PC9GR cells. The underlying mechanism involved in PC9GR cells resistant to osimertinib is unclear. Our results indicated that the overexpression of c-Met at least partially contributed to osimertinib resistance of PC9GR cells.

Furthermore, the expression levels of c-Met, AKT, ERK and GSK3β in PC9GR cells were found to be higher than those in PC9 cells (Fig. 3A). Unlike that in parental PC9 cells, the phosphorylation of AKT, ERK and GSK3β in the PC9GR cells was maintained in the presence of gefitinib (Fig. 3B), while the combination of gefitinib and Dic achieved a synergistic effect on the phosphorylation inhibition of c-Met, AKT, ERK and GSK3β in PC9GR cells (Fig. 3C), as well as the inhibition of their phosphorylation response to HGF in PC9GR cells (Fig. 3D).

We next examined the status of c-Met, EGFR, ERK, AKT and GSK3β in PC9 and PC9GR cells in the absence and presence of osimertinib. As shown in Fig. 3E, treatment with 2 μM osimertinib for 24 h markedly suppressed the expression the c-Met and the phosphorylation of c-Met and ERK in PC9 parent. Unexpectedly, osimertinib promoted the expression and phosphorylation of EGFR, enhanced c-Met phosphorylation without affecting c-Met expression nor the phosphorylation of ERK, AKT and GSK3β in PC9GR cells (Fig. 3F). Notably, Dic significantly inhibited EGFR expression and the phosphorylation of EGFR and c-Met induced by osimertinib in PC9GR cells (Fig. 3G).

### 3.3. Dic suppresses the stemness, invasiveness and migration of A549 cells and PC9GR cells.

We assessed the effects of Dic on the multiple properties linked to lung cancer metastasis. Lung cancer cell populations are highly heterogeneous and contain cancer stem-like cells which facilitate therapeutic resistance and tumor recurrence [14]. We next investigated the effect of Dic on the stemness of A549 cells via colony formation and sphere formation assays. As shown in Fig. 4A, Dic exhibited a strong inhibition of colony formation in a dose-dependent manner in A549 lung cancer cells which were cultured at low density and allowed to grow and form colonies over a two-week period. Furthermore, Dic showed an equivalent efficacy to that of a combined treatment with gefitinib and Dic in inhibiting the colony formation of PC9GR cells (Fig. 4B). Significantly decreased sphere diameter as well as sphere numbers under all tested concentrations was observed in the Dic treated groups in comparison with controls (Fig. 4C). Additionally, Dic substantially inhibited the expression of CD44 which has been recognized as a cell surface marker for stem cells (Fig. 4C). Thus, Dic treatment reduces the population of lung cancer cells with typical cancer stem-like phenotype.

The potential effect of Dic on A549 cell invasion and migration was tested and results from the transwell assay and matrigel transwell assay indicated that Dic could potently inhibit A549 cell migration and invasion, respectively (Fig. 4D). Additionally, a single dose Dic (100 μM) was as effective as a combination treatment with Dic and gefitinib in blocking the migration of PC9GR cells (Fig. 4E). Performing a scratch wound-healing assay, we further confirmed that treatment with Dic dose-dependently inhibited wound closure in A549 cells (Fig. 4F). Together, these results demonstrate that Dic inhibits in vitro the colony and sphere formation, migration and invasion of A549 cells.

### 3.4. Dic inhibits the adhesive ability and epithelial-mesenchymal transition (EMT) of A549 cells

Since cell-extracellular matrix (ECM) adhesion is required for the migration and spreading of cancer cells, we assessed the effect of Dic on the ability of A549 cells to adhere to collagen and fibrinogen. Results showed that Dic markedly inhibited the adhesion of A549 cells to collagen and fibrinogen in a dose-dependent manner (Fig. 5A).

Furthermore, as an important downstream effector of the c-Met signaling pathway, the focal adhesion kinase (FAK) plays a critical role in regulating cell adhesion and the expression of matrix metalloproteinase-2 (MMP-2)/MMP-9 to promote the migration and

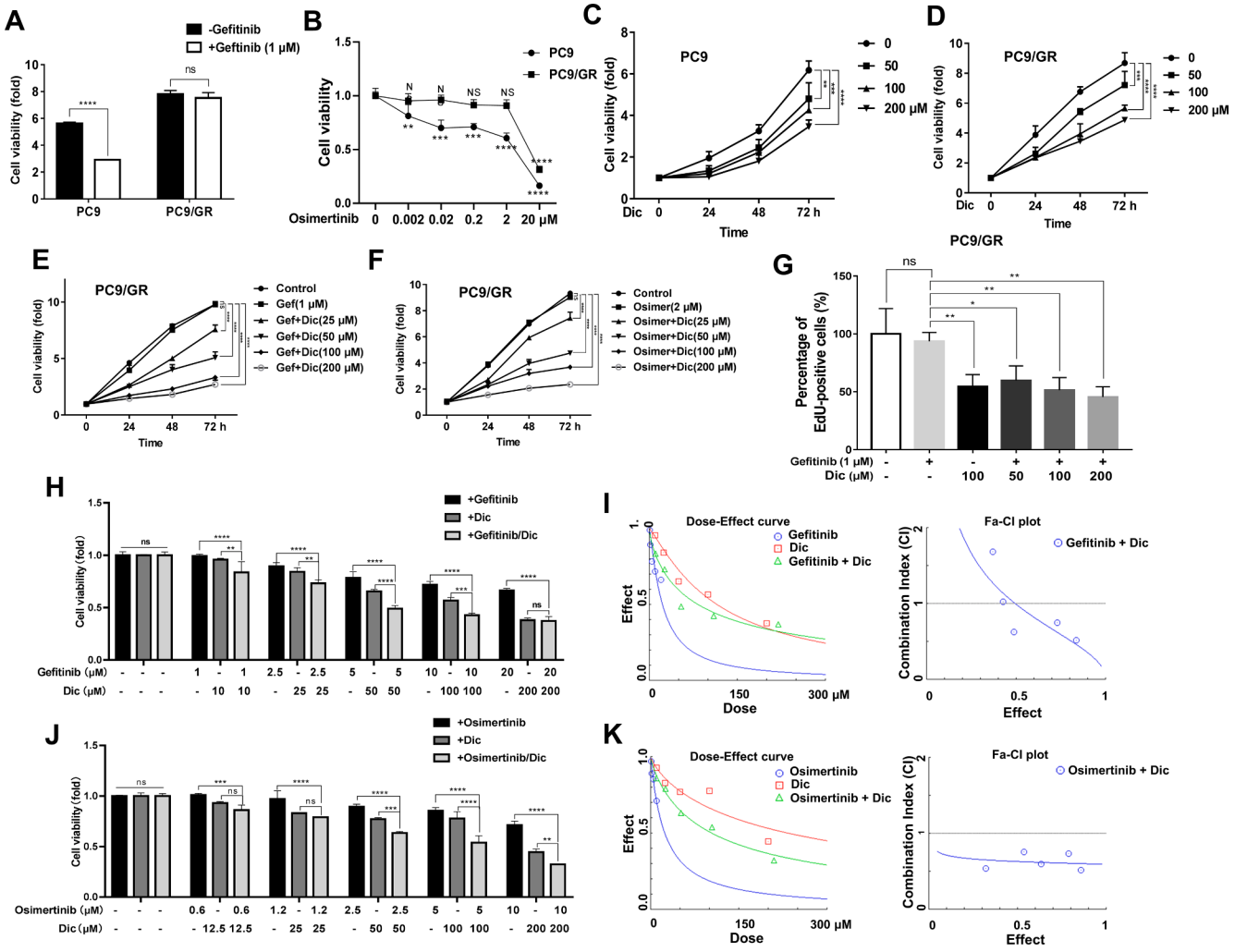


**Fig. 2. Dic synergistically enhanced cytotoxicity of gefitinib and osimertinib on PC9GR cells.** Comparison of the sensitivity of PC9 cells and PC9GR cells to gefitinib (Gef) (**A**) and osimertinib (Osimer) (**B**). Cell viability was assessed by CCK8 assay after treatment with gefitinib (Gef) (1 μM) or indicated concentrations of osimertinib (Osimer) for 72 h. PC9 (**C**) and PC9GR cells (**D**) were treated with various concentrations of Dic for the indicated times, following which cell proliferation was analyzed using the CCK8 assay (n = 3). (**E, F**) Cell viability of PC9GR cells after treatment with 1 μM gefitinib (Gef) or 2 μM osimertinib (Osimer) and different concentrations of Dic was determined by CCK8 assay at the indicated time points. (**G**) EdU incorporation assays were applied to examine the EdU positive PC9GR cells after treatment with gefitinib (Gef) (1 μM) and Dic for 48 h. (**H**) Either gefitinib (Gef) (1–20 μM) or Dic (10–200 μM) alone or in combination at 1:10 (gefitinib: Dic) fixed molar ration treatment for 48 h. Cell proliferation was determined by CCK8 assay. (**I**) Combination index (CI) analysis of PC9GR cells treated with the combination of gefitinib (Gef) and Dic. (**J**) Either osimertinib (Osimer) (0.6–10 μM) or Dic (12.5–200 μM) alone or in combination at 1:20 (osimertinib:Dic) fixed molar ration treatment for 48 h. Cell proliferation was determined by CCK8 assay. (**K**) Combination index (CI) analysis of PC9GR cells treated with the combination of osimertinib (Osimer) and Dic. A CI value of 1.0 (gray line) reflects additive effects, whereas values greater than and<1.0 indicate antagonism and synergy, respectively. Data were obtained from three independent experiments and represented as the mean ± S.D., **P < 0.01, ***P < 0.001, ****P < 0.0001 and ns (not significant) as compared with the controls.

**Table 4**
Combination index (CI) values for Gefitinib and Dic in combination.

| Cell line | Gefitinib (μM) | Dic (μM) | Molar ratio (Gefitinib:Dic) | Fa | CI |
|---|---|---|---|---|---|
| PC9GR | 1.0 | 10.0 | 1:10 | 0.83702 | 0.51733 |
| | 2.5 | 25.0 | | 0.73217 | 0.74711 |
| | 5.0 | 50.0 | | 0.48920 | 0.62996 |
| | 10.0 | 100.0 | | 0.42755 | 1.02223 |
| | 20.0 | 200.0 | | 0.37192 | 1.68201 |

**Table 5**
Combination index (CI) values for Osimertinib and Dic in combination.

| Cell line | Osimertinib (μM) | Dic (μM) | Molar ratio (Osimertinib:Dic) | Fa | CI |
|---|---|---|---|---|---|
| PC9GR | 0.6 | 12.5 | 1:20 | 0.86048 | 0.51603 |
| | 1.25 | 25 | | 0.79006 | 0.73537 |
| | 2.5 | 50 | | 0.63424 | 0.59477 |
| | 5 | 100 | | 0.53869 | 0.75920 |
| | 10 | 200 | | 0.32327 | 0.54320 |

invasion of cancer cells [15,16]. As shown in Fig. 5B, Dic efficiently inhibited the phosphorylation of FAK at Tyr-397 and Ser-722, and a major FAK substrate paxillin at Tyr-118 to suppress their activity, whereas Dic had no obvious effect on FAK protein expression and Src phosphorylation level. Additionally, Dic strongly counteracted HGF-induced MMP2/MMP9 expression in A549 cells (Fig. 5C). Taken together, these results suggest that inhibition of metastasis-related properties by Dic is related, at least in part, to the inhibition of cell adhesion and FAK activation.

It is well known that EMT plays an important role in cancer

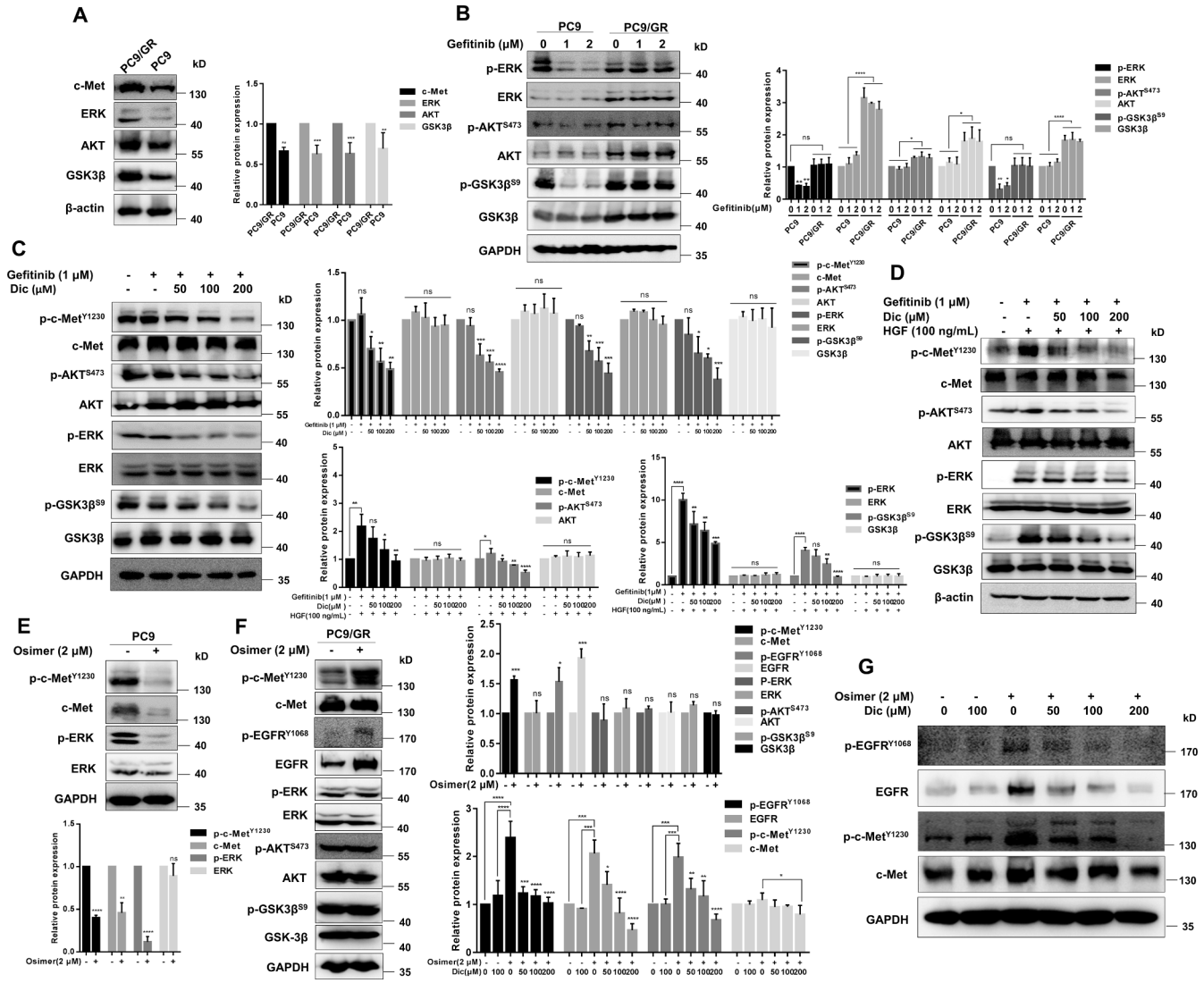


**Fig. 3. The synergistic effects of Dic and gefitinib or osimertinib on the inhibition of c-Met and EGFR signaling pathways in PC9GR cells.** (**A**) The expression levels of c-Met, ERK, Akt and GSK3β in PC9GR cells and PC9 cells. (**B**) The lung cancer cells were treated with different concentrations of gefitinib for 24 h, the expression level and phosphorylation levels of ERK, Akt and GSK3β were examined by Western blotting analysis. (**C**) The synergistic effects of gefitinib and Dic on the inhibition of phosphorylation of various MAPK and PI3K/Akt/mTOR signaling pathways components. PC9GR cells were treated with gefitinib and different concentrations of Dic for 36 h, then the phosphorylation levels of c-Met, Akt, ERK and GSK3β were detected by Western blotting analysis. (**D**) The synergistic effects of gefitinib (1 μM) and Dic on HGF-induced activation of c-Met signaling pathways in PC9GR cells. PC9GR cells were treated with gefitinib (1 μM) and indicated concentrations of Dic for 24 h in the absence of fetal bovine serum, following stimulation with 100 ng/ml HGF for 5 min, and indicated proteins were analyzed by Western blotting. (**E**) The expression and phosphorylation levels of c-Met and ERK in PC9 cells after treatment with 2 μM osimertinib for 24 h. (**F**) PC9GR cells were treated with 2 μM osimertinib for 24 h, the expression and phosphorylation levels of c-Met, EGFR, ERK, Akt and GSK3β were examined by Western blotting analysis. (**G**) The effect of Dic on the inhibition of c-Met and EGFR phosphorylation induced by osimertinib in PC9GR cells. Cells were treated with 2 μM osimertinib and different concentrations of Dic for 36 h, then the expression and phosphorylation levels of c-Met and EGFR were detected by Western blotting analysis. Images presented are representative of at least three independent experiments, and data are expressed as the mean ± S.D. The significance was determined by one-way ANOVA with Dunnett's test and *P < 0.05, **P < 0.01, ***P < 0.001 and ****P < 0.0001 for the designated treatment versus the control. ns, no significant differences.

progression, and is associated with the enhanced cellular migration and a stem-like phenotype, so we further observed the anti-EMT activity of Dic in A549 cells by detecting the expression levels of the epithelial marker E-Cadherin and mesenchymal markers N-Cadherin and Vimentin. During EMT, the expression of epithelial marker E-Cadherin is suppressed, while the expression of mesenchymal markers N-Cadherin and Vimentin is upregulated. As shown in Fig. 5D, quantitative PCR revealed that Dic significantly inhibited the mRNA expression levels of N-Cadherin and Vimentin, while E-Cadherin mRNA expression was stimulated by Dic. Similar results were also observed when TGF-β was used to induce EMT (Fig. 5E).

As shown in Fig. 5F, a more epithelial-like phenotype was acquired by A549 cells with the increasing Dic concentration, Dic treatment resulted in the upregulation of epithelial-like marker E-Cadherin as well as the downregulation of mesenchymal-like markers N-Cadherin and Vimentin. Moreover, when TGF-β was used to stimulate the EMT process, we found that Dic abolished TGF-β-induced E-Cadherin suppression and the expression of N-Cadherin and Vimentin (Fig. 5G). These results indicate that Dic efficiently inhibits EMT phenotypes.

### 3.5. *Validation of c-Met as a protein target of Dic*

The cellular thermal shift assay (CETSA) is a newly-developed fast method to assess the binding affinity of drugs to targeted proteins in

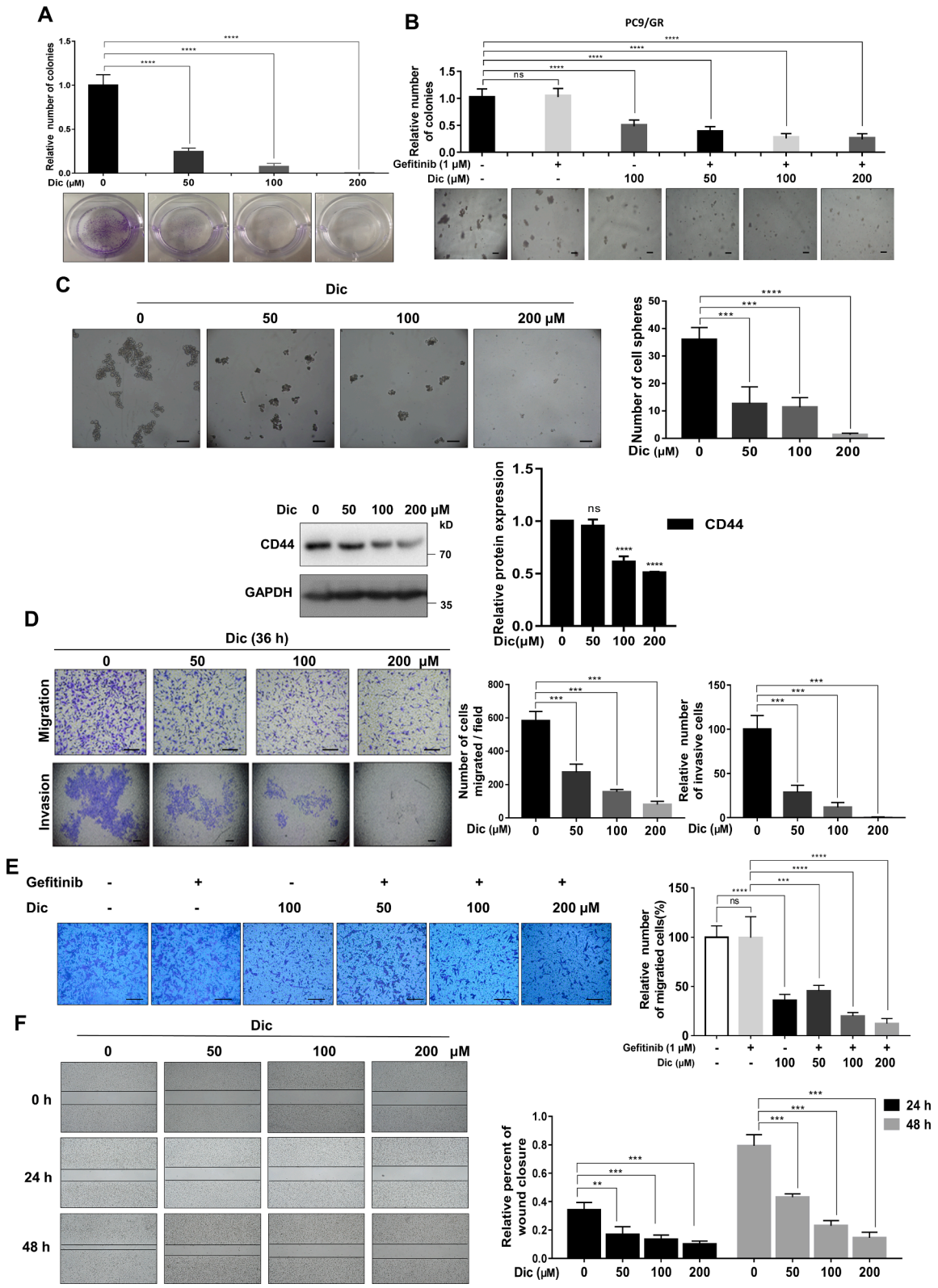


**Fig. 4. Dic suppresses the stemness, invasiveness and migration of A549 cells and PC9GR cells.** (**A**) Effect of Dic on the plate colony formation of A549 cells. Cells were treated with Dic and incubated for 2 weeks, colony numbers were counted using a microscope and the Image-Pro plus software program. (**B**) Effect of gefitinib and Dic on the soft agar colony formation of PC9GR cells. Cells were treated with gefitinib (1 μM) and different concentrations of Dic and incubated for 3 weeks. Scale bar = 200 μm. (**C**) After treatment with various concentrations of Dic for 48 h, A549 cells were subjected to the tumor sphere-forming assay. Scale bar = 200 μm. Expression of CD44 in A549 cells exposed to the indicated concentrations of Dic for 24 h was determined by Western blotting. (**D**) The effect of Dic on A549 cell migration and invasion were tested by using transwell assay (**D**, upper panel) and matrigel transwell assay (**D**, lower panel), respectively. Scale bar = 80 μm. (**E**) The effect of gefitinib and Dic on PC9GR cells migration was tested by transwell assay. Scale bar = 80 μm. (**F**) The effect of Dic on A549 cell migration was further tested by scratch wound-healing assay. Data shown as the mean ± S.D. For each assay, n = 3, the significance was determined by one-way ANOVA with Dunnett's test and $^{**}P < 0.01$, $^{***}P < 0.001$ and $^{****}P < 0.0001$ compared with the controls, ns, not significant.

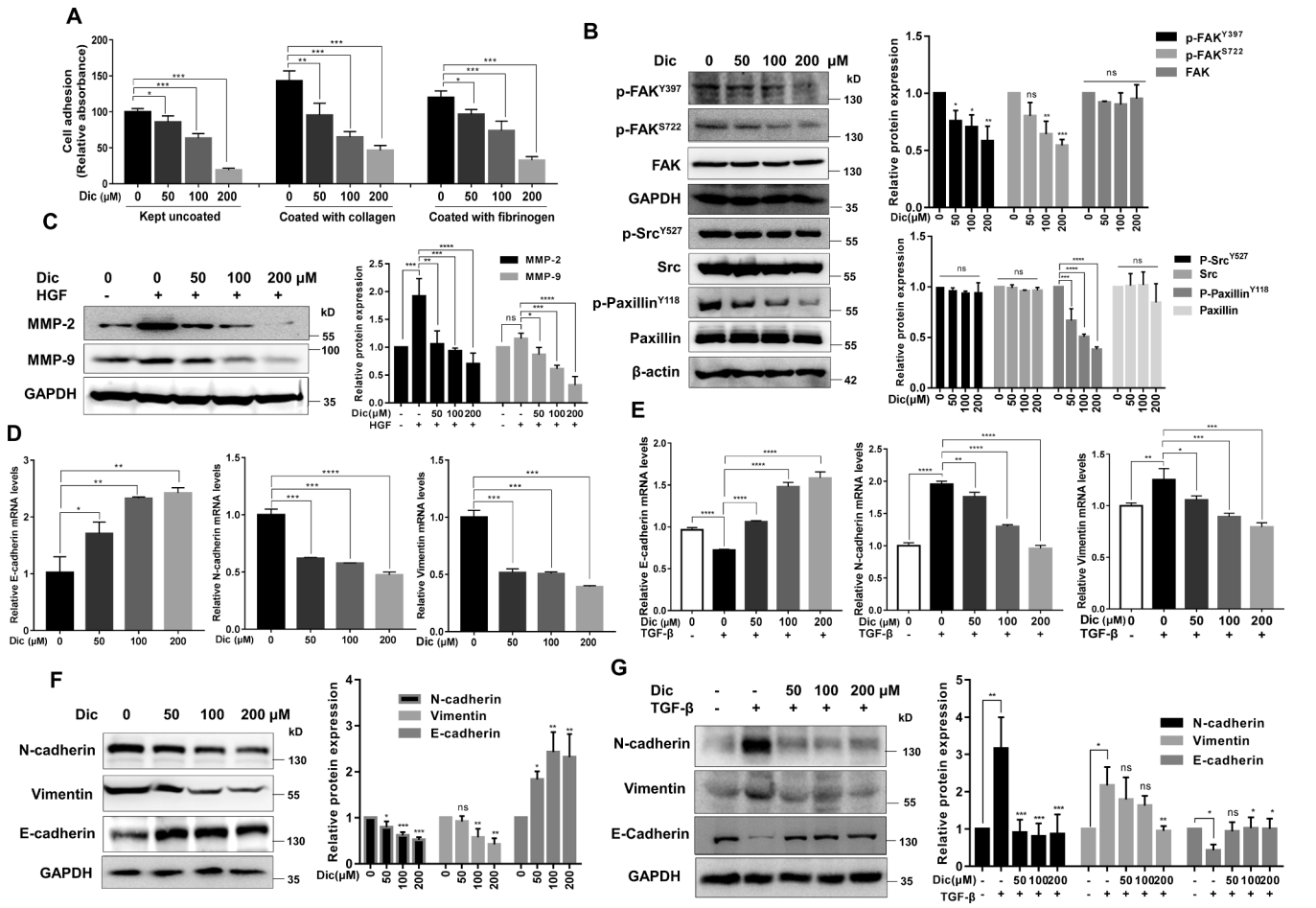


**Fig. 5. Dic inhibits the adhesive ability, MMP2/MMP9 expression and EMT in A549 cells.** (**A**) A549 cells treated with the indicated concentrations of Dic for 24 h were seeded into 96-well plates pre-coated with different ECM proteins (10 μg/mL collagen and 10 μg/mL fibrinogen). Wells coated with 100 μg/mL poly-L-lysine were employed as a control condition. The attached cells were fixed and stained with 0.1% crystal violet. Absorbance of dye was measured at 590 nm by using a microplate reader. Each bar represented as the mean ± S.D. (n = 3), and was expressed as a percentage of the control. *P < 0.05, **P < 0.01 and ***P < 0.001 compared with untreated group. (**B**) A549 cells were treated with various concentrations of Dic for 6 h, the phosphorylation levels of FAK at Tyr-397 and Ser-722, Src at Tyr-527 and paxillin at Tyr-118 were measured by Western blotting. (**C**) The effect of Dic on the HGF-induced MMP2/MMP9 expression. Cells were treated with different concentrations of Dic in the presence of 100 ng/ml HGF for 24 h. MMP2/MMP9 protein expression was determined by Western blotting. A549 cells were treated with different concentrations of Dic in the absence (**D**) or presence (**E**) of TGF-β (3 ng/mL) for 72 h. The mRNA expression levels of N-Cadherin, Vimentin and E-Cadherin were quantified by qRT-PCR normalized with GAPDH. The data were represented as the mean ± S.D. of three experiments. *P < 0.05, **P < 0.01, ***P < 0.001 and ****P < 0.0001 compared with the control group or the TGF-β-treated group. A549 cells were treated with different concentrations of Dic in the absence (**F**) or presence (**G**) of TGF-β (3 ng/mL) for 72 h. the expression levels of N-Cadherin, Vimentin and E-Cadherin were examined by Western blotting. Images shown are representative of at least three independent experiments, GAPDH expression was used as the loading control, and data are expressed as the mean ± S.D. *P < 0.05, **P < 0.01, ***P < 0.001 and ****P < 0.0001 when compared with the control group.

cells, and it is based on thermal stabilization of target proteins after binding by their ligands [10]. To identify whether Dic directly binds to c-Met, CETSA was employed to validate the binding of Dic to c-Met in A549 cell lysates. As shown in Fig. 6A, Dic treatment significantly enhanced the thermal stability of c-Met in the supernatant fraction. Next, to test whether Dic binds to c-Met in intact A549 cells, A549 cells treated with Dic or DMSO were collected, lysed and heated. In comparison with the control groups, Dic incubation resulted in a markedly increased thermal stability of c-Met at different temperatures (Fig. 6B) in a dose-dependent manner (Fig. 6C). Moreover, to investigate the incubation time effects, we treated A549 cells with Dic for the indicated time periods, while the concentration of Dic, time of heating and temperature were kept constant. A time-course experiment indicated that after 2 to 3 h, c-Met was saturated with Dic (Fig. 6D).

Additionally, the binding of a drug to its target protein can induce conformational changes which increase proteolytic stability of the target protein by decreasing its protease sensitivity. Therefore, we performed a drug affinity response target stability (DARTS) assay to test whether Dic directly binds to and stabilizes c-Met. As shown in Fig. 6E and F, the pre-incubation of Dic with A549 cell lysate effectively protected c-Met from digestion, even at pronase to protein ratios of 1:4000 and 1:3000. In addition, Dic stabilized c-Met in a dose-dependent manner as shown by an increase in the abundance of c-Met bands. Particularly, 100 and 200 μM of Dic noticeably protected c-Met from digestion in comparison with vehicle control. Furthermore, we also analyzed the binding sites for Dic in c-Met with a molecular docking study. Using the final computational docking model, we found that there were several hydrogen bonds formed between Dic and c-Met (Fig. 6G). The structural modeling of Dic with MET indicated that the tricyclic ring of Dic occupies the ATP-binding site in a predominantly hydrophobic environment formed by Ile-1084, Val-1092, Ala-1108, Lys-1110, Leu-1140, Tyr-1159, Met-1160, Met-1211 and Ala-1221, and Dic can form hydrogen bonds with two amino acids (Ile-1084 and Met-1160) of them. Additionally, Dic can also form hydrogen bond with Pro-1158. Pro-1158 has been characterized to play a vital role in stabilization of enzyme-inhibitor by donating hydrogen bond to the lactam amide nitrogen of a c-Met inhibitor, a

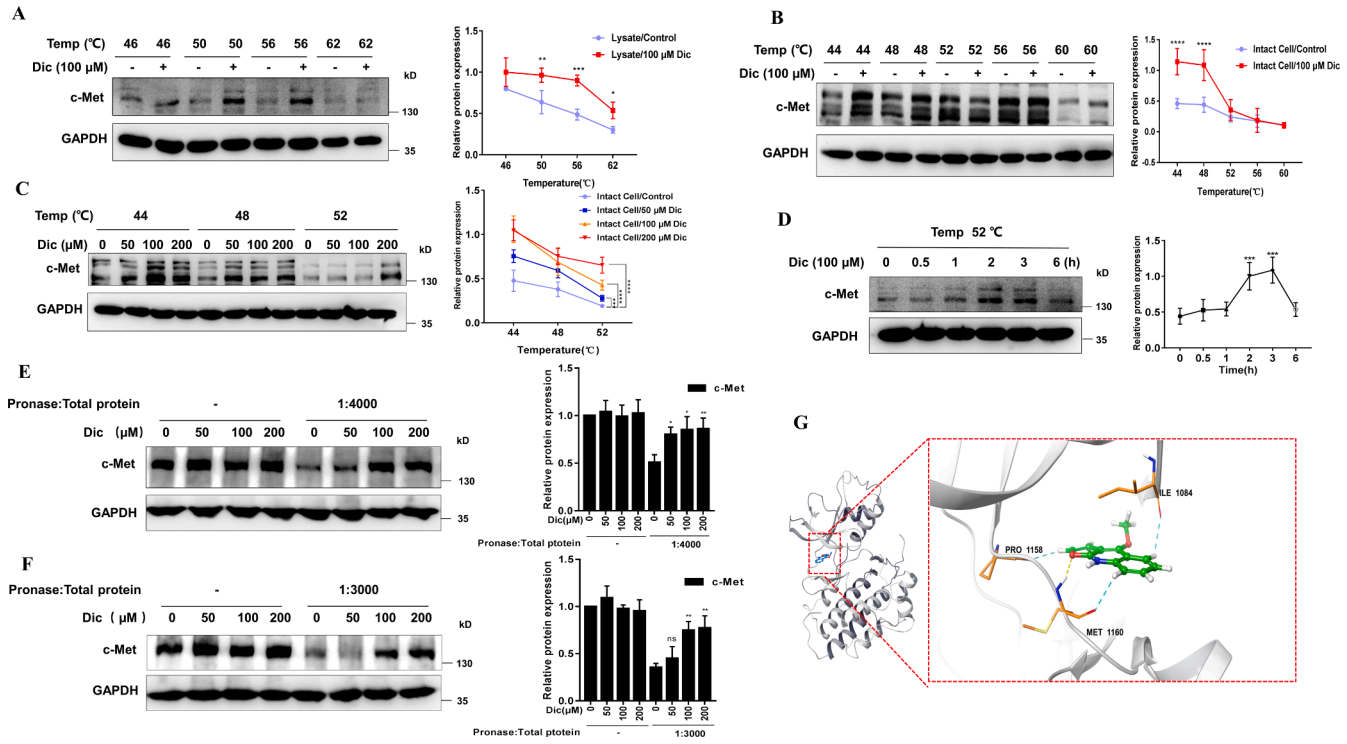


**Fig. 6. Validation of c-Met as a target protein of Dic by CETSA, DARTS and molecular docking.** (**A** and **B**) CETSA was performed on A549 cell lysates (**A**) and intact A549 cells (**B**) treated with the same concentration of Dic and heated to different temperatures. (**C**) For cell-based CETSA at different concentrations of Dic, A549 cells were treated with different concentrations of Dic for 2 h and then collected and lysed. The abundance of c-Met in the soluble fraction of cell lysates at different concentrations of Dic and different temperatures were analyzed. (**D**) Time course for CETSA in intact A549 cells. A549 cells incubated with 100 μM of Dic for the indicated time periods were heated at 52 °C for 3 min. The presence of c-Met in the soluble fraction of the cell lysates at different incubation periods was analyzed. The band intensity of c-Met and GAPDH was quantified by ImageJ software, the abundance of c-Met normalized to GAPDH is presented. (**E** and **F**) The DARTS assay was used to evaluate Dic's ability to bind to and stabilize c-Met. A549 cell lysates were incubated with Dic or vehicle at indicated concentrations for 2 h at room temperature, followed by digestion with pronase (pronase to protein ratio, 1:3000 or 1:4000) for 20 min at room temperature and analysis by Western blotting. The results shown are representative of three independent experiments, GAPDH expression was used as the loading control. All data represent the mean ± S. D. of at least three experiments, *P < 0.05, **P < 0.01, ***P < 0.001 and ****P < 0.0001 were calculated based on comparison with the control (one-way ANOVA with Dunnett's test). (**G**) Structural modelling of the Dic and c-Met interaction. The c-Met structure is shown as a ribbon representation and Dic is shown in stick form, the hydrogen bonds that formed between c-Met and Dic are shown as dotted lines.

microbial alkaloid compound [17]. In short, these data demonstrate that Dic potently and selectively binds to c-Met.

### 3.6. Inhibitory effects of Dic on c-Met signaling pathway

c-Met has been reported to control a wide variety of cellular processes including proliferation, differentiation and survival by regulating the PI3K/AKT/mTOR and MAPK signaling pathways. To evaluate the specific inhibitory effect of Dic on c-Met and elucidate the mechanisms responsible for the inhibitory effect of Dic on cancer cells with c-Met overexpression, we tested the influence of Dic treatment on the phosphorylation levels of major components of PI3K/AKT/mTOR and MAPK pathways, and also observed the influence of Dic on the activity or expression level of major downstream substrates and transcription factors regulated by these two pathways.

As shown in Fig. 7A, the tyrosine phosphorylation of c-Met in a control culture of A549 cells was obviously detectable, whereas c-Met phosphorylation was markedly suppressed in the cells treated with Dic in a dose-dependent manner. When A549 cells were treated with various concentrations of Dic for 36 h, the phosphorylation of B-Raf, C-Raf and ERK, recognized as the core components of MAPK signaling pathway (Fig. 7B), the phosphorylation of PI3K, AKT and mTOR, and the phosphorylation of transcription factor signal transducer and activator of transcription 3 (STAT3) regulated by MAPK and PI3K/AKT/mTOR pathway were significantly decreased in comparison with the controls (Fig. 7C).

Furthermore, when A549 cells were treated with indicated concentrations of Dic in serum-free medium for 24 h, following stimulation with or without 100 ng/mL HGF for 5 min, we found that cells stimulated with HGF alone exhibited higher phosphorylation levels of c-Met, PI3K, AKT, mTOR and GSK3β than cells from control group. Treatment with Dic led to a concentration-dependent inhibition of c-Met, PI3K, AKT, mTOR and GSK3β phosphorylation in response to HGF in A549 cells (Fig. 7D). GSK3β is a major substrate of AKT which inhibits GSK3β activity by phosphorylating its N-terminal serine to form an auto-inhibitory pseudosubstrate domain [18]. Additionally, GSK3β plays an important role in the cross-talk between PI3K/AKT/mTOR and Wnt/β-catenin signaling pathways [19].

Among the many well-known transcription factors regulated by PI3K/AKT and MAPK pathways are β-catenin, cyclin-D1, c-Myc and STAT3 [20-24]. Therefore, we assessed the effects of Dic on the activity of downstream transcription factors of PI3K/AKT and MAPK pathways to further understand the mechanisms by which Dic inhibits the proliferation of lung cancer cells. As shown in Fig. 7E, Dic strongly inhibited the expression of β-catenin, cyclin-D1, CDK1 and c-Myc as well as the phosphorylation of GSK3β. Notably, Dic treatment essentially inhibited the nuclear translocation of β-catenin, STAT3 and p-STAT3 in a dose-dependent manner (Fig. 7F).

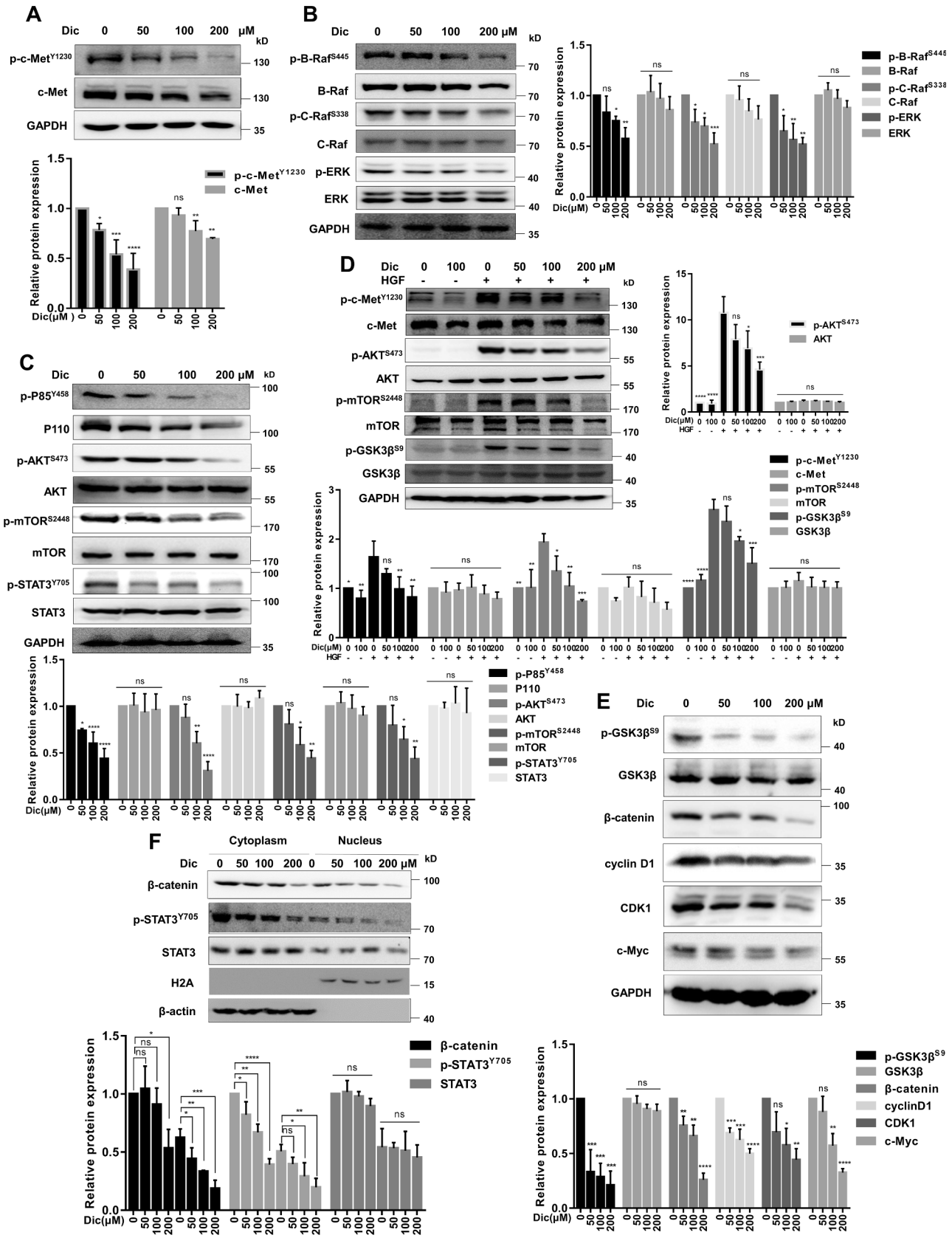


(caption on next page)

**Fig. 7. Dic is a potent c-Met inhibitor and suppresses the c-Met signaling pathway.** (**A**) The effect of Dic on the phosphorylation level of c-Met in A549 cells. Cells were treated with various concentrations of Dic for 36 h and analyzed by Western blotting. The effect of Dic on the inhibition of various MAPK (**B**) and PI3K/Akt/mTOR (**C**) signaling pathway components, cells were treated as described in (**A**). (**D**) Dic inhibited HGF-induced activation of c-Met signaling pathways in A549 cells. A549 cells were treated with the indicated concentrations of Dic for 24 h in the absence of fetal bovine serum following stimulation with or without 100 ng/mL HGF for 5 min and indicated proteins were analyzed by Western blotting. (**E**) The effect of Dic on the expression of p-GSK3β, transcription factors (β-catenin, cyclin D1 and c-Myc) and cell cycle-related proteins (cyclin D1 and CDK1). Cells were treated with various concentrations of Dic for 36 h and then the indicated proteins were detected. (**F**) The effect of Dic on the nuclear translocation of β-catenin, p-STAT3 and STAT3. Cells were treated with various concentrations of Dic for 36 h and then the distribution of β-catenin, p-STAT3 and STAT3 between cytoplasm and nucleus was observed by Western blotting. The results shown are representative of at least three independent experiments, GAPDH expression was used as the loading control. Each bar represents the mean ± S.D. **P < 0.01 and ****P < 0.0001 were calculated based on comparison with the control (one-way ANOVA with Dunnett's test).

### *3.7. Dic induces intrinsic apoptosis by activating caspase-7 and regulating the expression of pro- and anti-apoptotic proteins*

Since decreased PI3K/AKT and MAPK signaling pathways have been reported to cause apoptosis [25], we sought to test whether the retardation of cell proliferation in response to Dic treatment reflected cell apoptosis, and so we analyzed cell apoptosis in response to various Dic concentrations (0, 50, 100 and 200 μM) for 24 h. Dual Hoechst 33342/PI staining and TUNEL staining showed that Dic promoted the apoptosis of A549 cells (Fig. 8A and B). Next, we assessed the mRNA

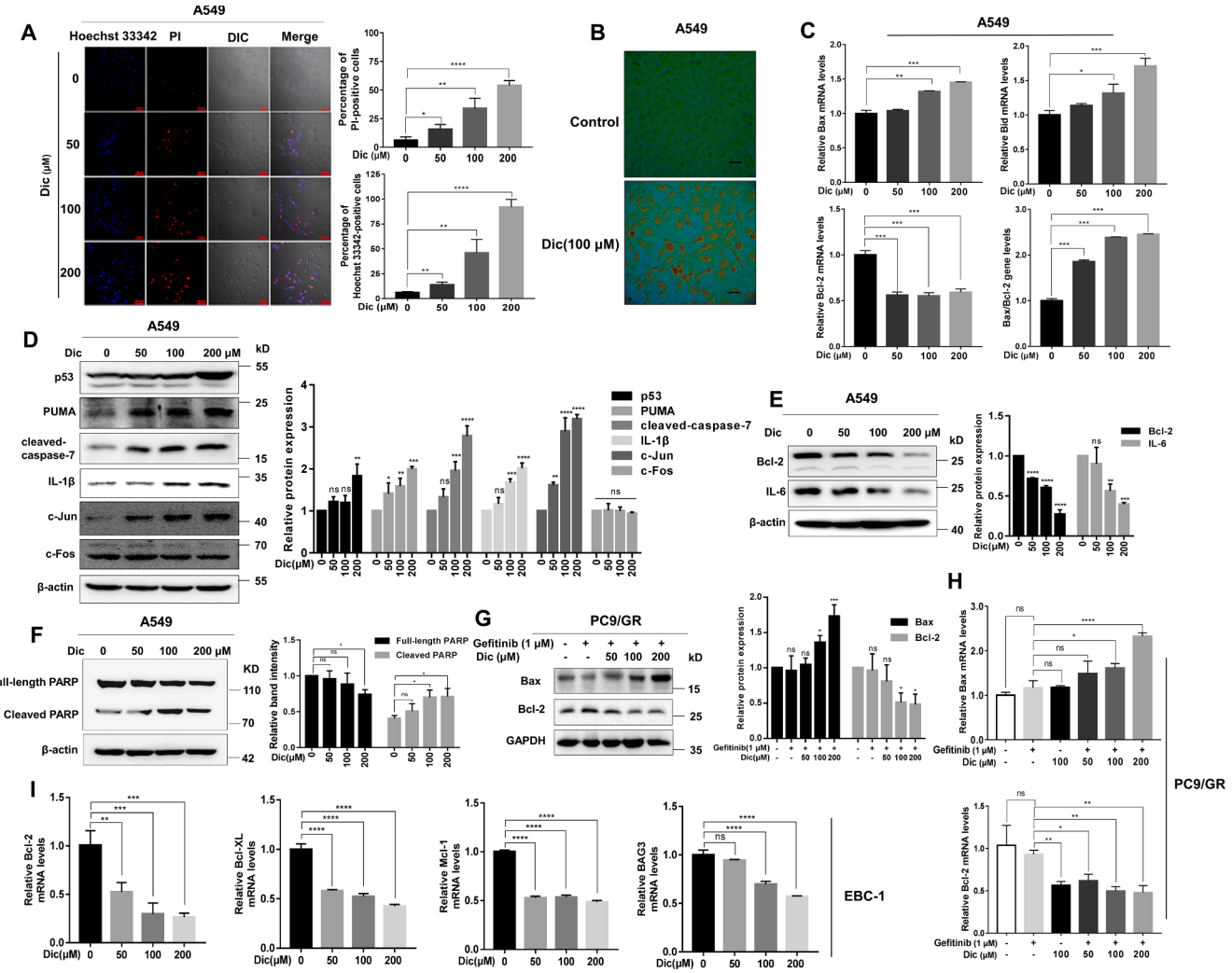


**Fig. 8. Dic induces intrinsic apoptosis in A549, PC9GR and EBC-1 cells.** (**A**) A549 cells were exposed to different concentrations of Dic for 24 h and cell mortality was quantified by PI/Hoechst 33,342 staining. Scale bar = 80 μm. (**B**) TUNEL staining was performed to assess the apoptosis of A549 cells after treatment with Dic for 48 h. Scale bar = 100 μm. (**C**) The effect of Dic on the mRNA expression levels of Bax, Bid and Bcl-2 was determined by qRT-PCR normalized with GAPDH. The effect of Dic on the expression levels of pro-apoptotic proteins p53, PUMA, Bax, cleaved-caspase-7, IL-1β, c-Jun, c-Fos (**D**), and anti-apoptotic proteins Bcl-2 and IL-6 (**E**), and PARP-1 cleavage, an universal hallmark of apoptotic cell (**F**), were determined by Western blotting. For C-F, cells were treated as described in (**A**). (**G**) PC9GR cells were exposed to gefitinib (1 μM) and indicated concentrations of Dic for 24 h, the protein expression levels of Bax and Bcl-2 in PC9GR cells were determined by Western blotting. (**H**) The synergistic effects of gefitinib and Dic on the mRNA expression levels of pro-apoptotic protein Bax and anti-apoptotic protein Bcl-2 was determined by qRT-PCR normalized to GAPDH, cells were treated as described in (**G**). (**I**) EBC-1 cells were exposed to different concentrations of Dic for 48 h, and the effect of Dic on the mRNA expression levels of Bcl-2, Bcl-XL, BAG3 and Mcl-1 was determined by qRT-PCR normalized with GAPDH. For C-F, similar results were obtained from three independent experiments, GAPDH or β-actin expression was used as the loading control. All data are expressed as the mean ± S.D. of three experiments, *P < 0.05, **P < 0.01, ***P < 0.001 and ****P < 0.0001 were calculated based on comparison with the control (one-way ANOVA with Dunnett's test), ns, not significant.

expression of Bax, Bid and Bcl-2 in A549 cells by qRT-PCR analysis. The results revealed that Dic significantly upregulated the mRNA expression of pro-apoptotic proteins Bax and Bid and downregulated the mRNA expression of anti-apoptotic protein Bcl-2 in a dose-dependent manner (Fig. 8C).

Furthermore, Dic induced dose-dependent upregulation of p53, p53 upregulated modulator of apoptosis (PUMA), Bax, cleaved-caspase-7, IL-1β, c-Jun and PARP-1 cleavage expression, and downregulation of Bcl-2, and IL-6 expression. This is consistent with the pro-apoptotic functions of p53, PUMA, Bax, cleaved-caspase-7, IL-1β and c-Jun being activated and the anti-apoptotic functions of Bcl-2 and IL-6 being suppressed upon exposure to environment stress, whereas Dic had no detectable effect on the expression of c-Fos (Fig. 8D-F).

In addition, combined treatment with gefitinib and Dic had a synergistic promotional effect on the mRNA expression of Bax in PC9GR cells, and Dic alone exhibited an equivalent efficacy of both drugs in inhibiting Bcl-2 mRNA expression (Fig. 8H). The combined effects of Dic and gefitinib on the protein expression levels of Bax and Bcl-2 were confirmed by Western blotting (Fig. 8G). Notably, Dic also significantly inhibited the mRNA expression of anti-apoptotic proteins including Bcl2, Bcl-XL, BAG3 and Mcl-1 in c-Met-dependent EBC-1 cells (Fig. 8I).

### 3.8. Suppression of xenograft tumor growth by Dic administration

To further investigate the anti-tumorigenic potential of Dic, an A549 lung cancer xenograft model was employed to evaluate the inhibitory efficiency of Dic in vivo. A549 cells were injected subcutaneously into the right armpit of nude mice (n = 12), when the tumor volume reached 100–150 $mm^3$, the tumor-bearing mice were randomly divided into two groups (groups Dic and vehicle) with six mice per group. The Dic-treated group received an intraperitoneal injection of Dic (50 mg/kg) once a day for 15 consecutive days.

As shown in Fig. 9A and B, Dic significantly inhibited A549 cell growth when compared with that of the control group in vivo. Consistently, tumor volume increased rapidly in the control group compared with the treatment group (Fig. 9C). Additionally, treatment with Dic was well tolerated without notably body weight loss (Fig. 9D). H&E (Haemotoxylin and Eosin) staining results indicated that tumor cells in the control group were dense and uniform, and the cell nucleus was intensely stained, while nuclear pyknosis, fragmentation and broad dissolved necrotic area were observed in Dic-treated group (Fig. 9E). We then examined the effects of Dic on the Ki67 tumor proliferation marker by using immunohistochemistry. The expression of Ki67 was significantly decreased by treatment with Dic (Fig. 9E and F). To confirm the apoptosis-inducing effect of Dic in vivo, TUNEL staining was used in xenograft tumor tissue, a significantly higher number of TUNEL-positive cells was observed in Dic-treated group than in the control group (Fig. 9E-G).

## 4. Discussion

c-Met is a receptor tyrosine kinase (RTK) whose only known natural ligand is HGF. HGF binding promotes the dimerization of c-Met and activates signaling pathways including PI3K/AKT/mTOR, MAPK [3,26,27], the GSK3/β-catenin pathways, and enhances the expression of transcription factors such as STAT3 [28,29], c-Myc [30] and cyclin D1 [31]. Normal c-Met signaling plays a critical role in embryogenesis, liver generation [32] and wound healing [33] by regulating cell proliferation and differentiation. As a proto-oncogene, aberrant HGF/c-Met activation has been closely linked to the initiation and metastasis of various types of human cancers [26,34-36], especially NSCLC [3,37], through the regulation multiple biological processes such as tumor proliferation, metastasis, survival and EMT [26]. Aberrantly activated c-Met signaling can arise from the mutation of c-Met, amplification of MET, or c-Met overexpression due to increased HGF level which also mediates the acquired resistance of EGFR-TKIs such gefitinib in NSCLC [26,27]. Additionally, c-Met overexpression is observed in 61% of NSCLCs and is positively correlated with advanced stage, poor prognosis and poor survival in NSCLC [38].

Since c-Met is overexpressed in a wide range of tumors and is emerging as an important target for cancer therapy, a number of small molecule c-Met inhibitors have been developed over the past few decades. Two multi-target c-Met inhibitors, crizotinib and cabozantinib, have been approved by the U.S. Food and Drug Administration (FDA) for the treatment of locally advanced or metastatic NSCLC patients and patients with advanced renal cell carcinoma or hepatocellular carcinoma, respectively. However, most c-Met inhibitors currently being developed are multi-target inhibitors which may lead to unwanted side effects. Although monoclonal antibodies specifically target c-Met or HGF, they still face the same common disadvantages as other large biological molecules [3]. Thus, great efforts should be dedicated towards developing selective c-Met TKIs.

Dic, a naturally occurring furoquinoline alkaloid, has been reported to possess a wide range of beneficial pharmacological activities including anticancer activity against multiple tumor types. Dic has shown potent proliferation-inhibition and apoptosis-induced activities in various human cancer-derived cell lines such as cervix, colon and breast cancer cells [6]. Recently, Dic was reported to induce cell cycle arrest at low concentration and apoptosis at high concentration in lung cancer cells by mitochondria and caspase-3-independent mechanisms [7]. In addition, Dic was shown to inhibit the proliferation of colorectal carcinoma HCT 116 cell and promote HCT 116 apoptosis by down-regulating hypoxia inducible factor-1α (HIF-1α) and slug [39]. However, the detailed molecular mechanisms and the direct target by which Dic inhibits cancer cell proliferation and induces cancer cell apoptosis are still unclear.

In the present study, expectedly, Dic potently inhibited the proliferation of various types of cancer cell lines including A549, H1299, HepG2, ACHN and HeLa. All these cells possess a shared characteristic in that they display a strong c-Met expression [40-42], notably Dic showed no significant effect on the proliferation of HEK293 cells which have undetectable expression of c-Met. Next, we demonstrated that Dic is a potent inhibitor of c-Met based on the following evidence: (a) Dic blocked HGF-induced c-Met phosphorylation; (b) Dic inhibited HGF-induced A549 cell proliferation and the activation of c-Met signaling pathway; (c) CETSA, DARTS and molecular docking indicated that Dic directly interacted with c-Met.

Consistently with previous reports, we found that there is a higher expression of c-Met in both lung adenocarcinoma and squamous cell carcinoma of lung compared with normal tissue as determined by bioinformatics analysis, Western blotting and qRT-PCR. In addition to proliferation inhibition, we also found that Dic treatment significantly inhibited the colony formation, migration, invasion, stemness, adhesive ability, EMT and in vivo xenograft tumor growth of A549 lung cancer cells. When exploring the mechanisms involved in Dic's effect on A549 cells, the results demonstrated that Dic markedly suppressed the activation of PI3K/AKT/mTOR and MAPK signaling pathways, inhibited the expression of transcription factors including β-catenin, cyclin D1, c-Myc and STAT3 phosphorylation, and prevented the nuclear translocation of β-catenin, p-STAT3 and STAT3. Additionally, Dic was shown to promote the apoptosis of A549 cells via intrinsic apoptosis pathways. Furthermore, to the best of our knowledge, Dic is presently the smallest c-Met inhibitor with a molecular weight of 199.21 Da. Dic displayed a comparable potency to the other two c-Met inhibitors (savolitinib and crizotinib) against the proliferation of c-Met-dependent EBC-1 lung cancer cells. Notably, the combination of Dic and gefitinib or osimertinib synergistically inhibited the cell proliferation, induced apoptosis, and suppressed the PI3K/AKT/mTOR and MAPK signaling pathways in PC9GR cells.

It is well known that PI3K/AKT/ mTOR and MAPK signaling pathways are the two key pathways in c-Met-mediated signal transduction [3,26]. Abnormal c-Met signaling promotes the development and

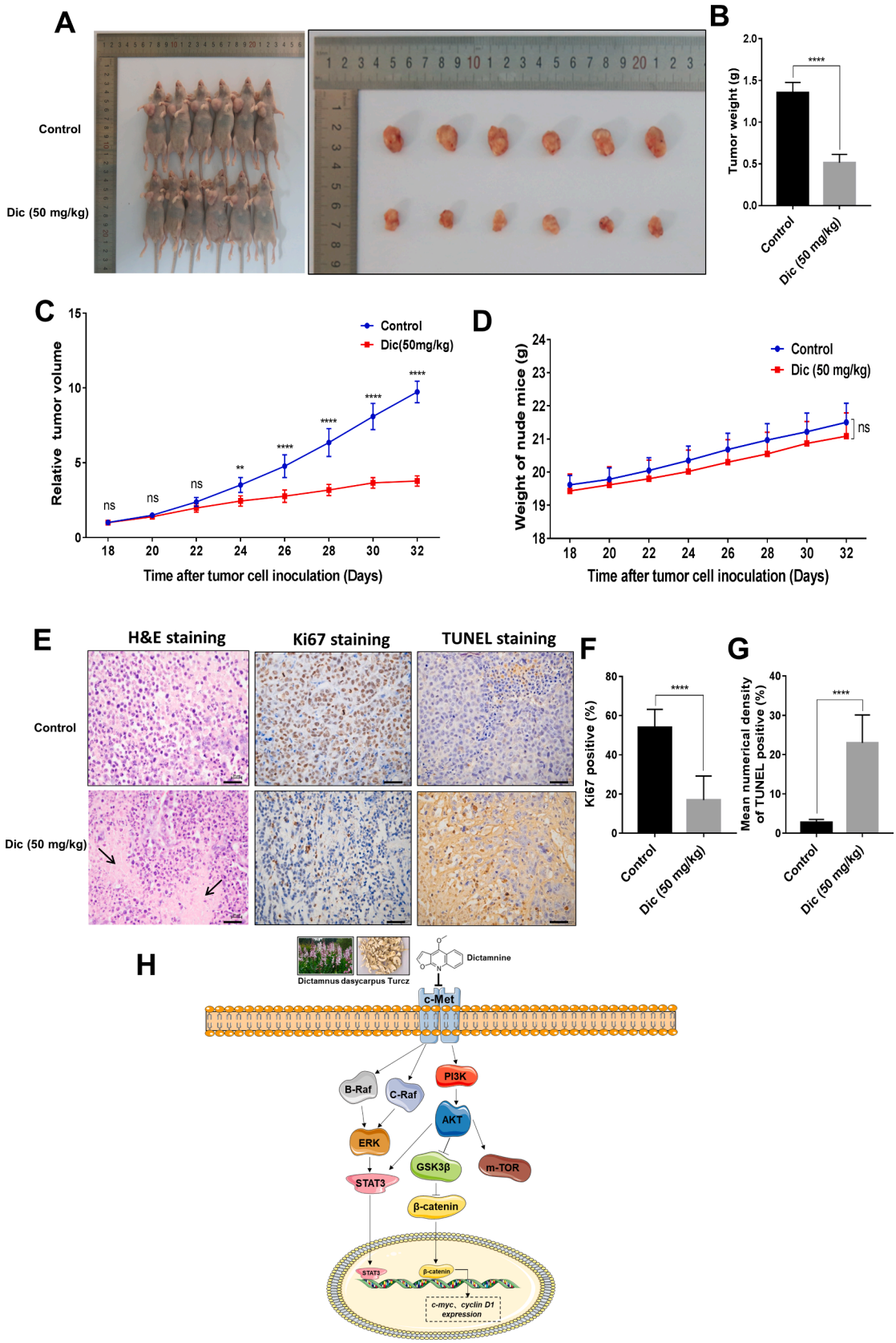


*(caption on next page)*

**Fig. 9. Effects of Dic on A549 growth in a xenograft mouse model.** (**A-G**) A549 cells ($5 \times 10^6$ cells/mice) were injected subcutaneously into the right armpits of mice. On the 9th day after inoculation, when the tumors reached a volume of 100–150 $mm^3$, two groups of tumor-bearing nude mice (n = 6, each group) were injected intraperitoneally with either Dic (50 mg/kg) or physiological saline (0.9% NaCl), respectively. After 15 days of consecutive injections, the mice were sacrificed. (**A**) Representative necropsy images of mice and dissected tumors are shown. (**B**) Tumor weight of dissected tumors from the two groups of mice was measured at the end of the experiment. The results are expressed as the mean ± S.D., ****P < 0.0001 compared with control (one-way ANOVA with Dunnett's test). (**C**) Tumor volumes were measured during the experiment, and these data are represented as the mean ± S.D., **P < 0.01 and ****P < 0.0001 compared with the control (one-way ANOVA with Dunnett's test). (**D**) Body weight changes in mice treated with Dic or vehicle. Data are represented as the mean ± S.D., ns, not significant. (**E**) Histological features were analyzed by H&E staining in sections from the tumors. (**E-G**), Immunohistochemical analysis was performed with sections of excised tumors. Each scale bar represents 30 μm, ****P < 0.0001 compared with control (one-way ANOVA with Dunnett's test). (**H**) Scheme of the proposed mechanism. This shows that Dic directly targets c-Met, leading to the downregulation of the PI3K/Akt/mTOR, MAPK signaling pathways and proliferation-related gene expression, eventually inhibiting lung cancer cell proliferation and tumor growth.

metastasis of NSCLC, and is associated with initial resistance and acquired resistance to EGFR-TKIs in patients with NSCLC [13,43]. Our results demonstrated that Dic treatment inhibited the phosphorylation of the key components of PI3K/AKT/mTOR pathway including PI3K, AKT and mTOR in the presence or absence of HGF, and also inhibited the phosphorylation of the key components of MAPK pathway including B-Raf, C-Raf and ERK1/2.

STAT3 is an important transcription factor, its persistent phosphorylation has been demonstrated in 22% ~ 65% of NSCLC. STAT3 can be activated by receptor tyrosine kinases such as c-Met in a Janus family kinase-mediated way [29,44]. c-Myc, one of the critical transcription factors, has been shown to be implicated in promoting the metastasis of many cancers, mainly through enhancing tumor growth and cancer cell survival [45]. c-Myc was found to function as the downstream effector of c-Met to drive cell growth in NSCLC and gastric cancer cells [30]. Cyclin D1 is an important cell cycle regulator and has been proved to be a mediator of c-Met-induced hepatocarcinogenesis [31]. It is noteworthy that both c-Myc and cyclin D1 are considered to be the major downstream target of β-catenin [46,47].

Furthermore, the c-Met signaling pathway is closely related to the Wnt/GSK3/β-catenin pathway and prevents the phosphorylation of β-catenin by GSK3, and this, in turn, promotes the nuclear translocation of β-catenin and enhance its transcriptional activity, facilitating tumorigenesis [48-50]. The phosphorylation level of GSK3β, β-catenin expression and its translocation from cytoplasm to nucleus were significantly inhibited in A549 cells after treatment with Dic.

β-catenin is the key component in the canonical Wnt pathway. When cells are not stimulated with Wnt ligand, β-catenin is maintained at low level due to phosphorylation by GSK, resulting in the ubiquitination and degradation of β-catenin. GSK is one of the first identified substrates of AKT kinase. GSK-activity is inhibited after phosphorylation by AKT due to the formation of an autoinhibitory pseudosubstrate domain in the N-terminus of GSK. Interestingly, AKT phosphorylates GSK and inhibits its activity, while the phosphorylation of β-catenin, as a GSK substrate, is not affected by changes of AKT activity [26,51]. Presently, it is known that β-catenin is phosphorylated by GSK inside the β-catenin destruction complex, and ubiquinated and degraded via the proteasome [52]. In fact, only a very small portion of GSK and β-catenin is involved in the formation of β-catenin destruction complex. More importantly, phosphorylated GSK in this complex still has the ability to phosphorylate β-catenin [18,52]. Thus, it is necessary to be very careful when interpreting the relationship between GSK phosphorylation level and the level of β-catenin. In this study, Dic not only inhibited GSK phosphorylation and downregulated the level of β-catenin, but also suppressed the nuclear translocation of β-catenin.

In this study, the concentrations of Dic used in in vitro experiments seem relatively high. However, to the best of our knowledge, the molecular weight of Dic (199.21 Da) is lower than that of currently reported c-Met inhibitors, and is also far lower than the average molecular weight of drugs (greater than 600 Da) approved by FDA in the past decade. Additionally, it is known that lower molecular weight implies higher molarity when the same dose is used.

Furthermore, Dic, as a bioactive natural furoquinoline compound, contains a quinoline ring and it is a very simple quinoline-based molecule. The quinoline ring system has long been recognized as a versatile nucleus used for the design and synthesis of bioactive compounds [53]. Currently, it is reported that more than one hundred quinoline compounds have been approved for the treatment of oncology and bacterial infections. Especially in the development of new anticancer agents, quinoline compounds have been designed to preferentially target c-Met, EGFR and VEGR, and more than 20 quinoline based c-Met inhibitors including cabozantinib and foretinib have been developed [54]. Dic, as a quinoline compound with a simple structure, would be considered to be a lead compound suitable for structure modification to further improve its pharmacological properties.

In this study, Dic has been found to inhibit c-Met phosphorylation as well as c-Met expression in EBC-1 cells. A number of studies have shown that c-Met expression and degradation are regulated at multiple layers through various mechanisms which are complex and unclear. c-Met expression in different cells is regulated through several independent mechanisms including regulation mediated by transcription factors (Sp1 and Ets-1), microRNAs, p53 pathway, EGFR pathway as well as regulation by c-Met itself [55]. Our q-PCR results have shown that the mRNA expression of c-Met in EBC-1 cells is downregulated by Dic in a dose-dependent manner, while the detailed molecular mechanisms involved in the inhibitory effect of Dic on c-Met mRNA expression in EBC-1 cells are currently unclear and warrant further investigation. Additionally, a recent study has shown that BPI-9016 M, a c-Met inhibitor, can also reduce the expression of c-Met in A549 and H1299 cells [42].

In summary, our results show that Dic directly binds to c-Met and inhibits its phosphorylation, which leads to the suppression of lung cancer growth in vitro and in vivo by the downregulation of PI3K/AKT/mTOR and MAPK signaling pathways (Fig. 9H). Notably, Dic and gefitinib or osimertinib exhibit synergistic effects on EGFR-TKI-resistant lung cancer cells. These findings together suggest the potential use of Dic as a potential therapeutic agent in the therapy of lung cancer or other cancers with overactive c-Met pathway.

*CRediT authorship contribution statement*

**Jiaojiao Yu:** Investigation, Writing – original draft, Writing – review & editing. **Lijing Zhang:** Investigation, Data curation. **Jun Peng:** Investigation, Data curation. **Richard Ward:** Writing – review & editing, Data curation. **Peiqi Hao:** Methodology, Validation. **Jiwei Wang:** Validation. **Na Zhang:** Validation. **Yang Yang:** Validation. **Xiaoxi Guo:** Validation, Funding acquisition. **Cheng Xiang:** Validation. **Su An:** Supervision, Writing – original draft, Writing – review & editing, Funding acquisition. **Tian-Rui Xu:** Supervision, Writing – review & editing, Funding acquisition.

## Declaration of Competing Interest

The authors declare that they have no known competing financial interests or personal relationships that could have appeared to influence the work reported in this paper.

## Acknowledgements

This research was funded by the National Natural Science Foundation of China (NSFC) (grant number 81760264, 81960394 and 81960659), the Key Fund of Yunnan Basic Research Program (grant number 202001AS070024), the National Key Research and Development Project (grant number 2018YFA0801404) and conducted in the University Based Provincial Key Laboratory of Screening and Utilization of Targeted Drugs.

## References

[1] Z. Chen, C.M. Fillmore, P.S. Hammerman, C.F. Kim, K.K. Wong, Non-small-cell lung cancers: a heterogeneous set of diseases, Nat. Rev. Cancer 14 (8) (2014) 535–546.
[2] R. Romagnoli, F. Prencipe, P. Oliva, S. Baraldi, P.G. Baraldi, S. Schiaffino Ortega, M. Chayah, M. Kimatrai Salvador, L.C. Lopez-Cara, A. Brancale, S. Ferla, E. Hamel, R. Ronca, R. Bortolozzi, E. Mariotto, E. Mattiuzzo, G. Viola, Design, Synthesis, and Biological Evaluation of 6-Substituted Thieno[3,2- d]pyrimidine Analogues as Dual Epidermal Growth Factor Receptor Kinase and Microtubule Inhibitors, J. Med. Chem. 62 (3) (2019) 1274–1290.
[3] Y.-L. Wu, R.A. Soo, G. Locatelli, U.z. Stammberger, G. Scagliotti, K. Park, Does c-Met remain a rational target for therapy in patients with EGFR TKI-resistant non-small cell lung cancer? Cancer Treat. Rev. 61 (2017) 70–81.
[4] T. Fujino, K. Suda, T. Mitsudomi, Emerging MET tyrosine kinase inhibitors for the treatment of non-small cell lung cancer, Expert Opin. Emerg. Drugs 25 (3) (2020) 229–249.
[5] P. Wang, J. Sun, J. Xu, Q. Yan, E. Gao, W. Qu, Y. Zhao, Z. Yu, Pharmacokinetics, tissue distribution and excretion study of dictamnine, a major bioactive component from the root bark of Dictamnus dasycarpus Turcz. (Rutaceae), J. Chromatogr. B 942-943 (2013) 1–8.
[6] P. Wang, Y. Zhao, Y. Zhu, J. Sun, A. Yerke, S. Sang, Z. Yu, Metabolism of dictamnine in liver microsomes from mouse, rat, dog, monkey, and human, J. Pharm. Biomed. Anal. 119 (2016) 166–174.
[7] F.-F. An, Y.-C. Liu, W.-W. Zhang, L. Liang, Dihydroartemisinine Enhances Dictamnine-induced Apoptosis via a Caspase Dependent Pathway in Human Lung Adenocarcinoma A549 Cells, Asian Pac. J. Cancer Prev. 14 (10) (2013) 5895–5900.
[8] T.-C. Chou, Drug combination studies and their synergy quantification using the Chou-Talalay method, Cancer Res. 70 (2) (2010) 440–446.
[9] D. Yu, E. Kahen, C.L. Cubitt, J. McGuire, J. Kreahling, J. Lee, S. Altiok, C.C. Lynch, D.M. Sullivan, D.R. Reed, Identification of Synergistic, Clinically Achievable, Combination Therapies for Osteosarcoma, Sci. Rep. 5 (2015) 16991.
[10] D.M. Molina, R. Jafari, M. Ignatushchenko, T. Seki, E.A. Larsson, C. Dan, L. Sreekumar, Y. Cao, P. Nordlund, Monitoring Drug Target Engagement in Cells and Tissues Using the Cellular Thermal Shift Assay, Science 341 (6141) (2013) 84–87.
[11] K.V.M. Huber, K.M. Olek, A.C. Müller, C.S.H. Tan, K.L. Bennett, J. Colinge, G. Superti-Furga, Proteome-wide drug and metabolite interaction mapping by thermal-stability profiling, Nat. Methods 12 (11) (2015) 1055–1057.
[12] B. Lomenick, R. Hao, N. Jonai, R.M. Chin, M. Aghajan, S. Warburton, J. Wang, R. P. Wu, F. Gomez, J.A. Loo, J.A. Wohlschlegel, T.M. Vondriska, J. Pelletier, H. R. Herschman, J. Clardy, C.F. Clarke, J. Huang, Target identification using drug affinity responsive target stability (DARTS), Proc. Natl. Acad. Sci. U. S. A. 106 (51) (2009) 21984–21989.
[13] M.M. Awad, G.R. Oxnard, D.M. Jackman, D.O. Savukoski, D. Hall, P. Shivdasani, J. C. Heng, S.E. Dahlberg, P.A. Jänne, S. Verma, J. Christensen, P.S. Hammerman, L. M. Sholl, MET Exon 14 Mutations in Non-Small-Cell Lung Cancer Are Associated With Advanced Age and Stage-Dependent MET Genomic Amplification and c-Met Overexpression, J. Clin. Oncol. 34 (7) (2016) 721–730.
[14] L. MacDonagh, S.G. Gray, E. Breen, S. Cuffe, S.P. Finn, K.J. O'Byrne, M.P. Barr, Lung cancer stem cells: The root of resistance, Cancer Lett. 372 (2) (2016) 147–156.
[15] C. Zhang, S.R. Stockwell, M. Elbanna, R. Ketteler, J. Freeman, B. Al-Lazikani, S. Eccles, A. De Haven Brandon, F. Raynaud, A. Hayes, P.A. Clarke, P. Workman, S. Mittnacht, Signalling involving MET and FAK supports cell division independent of the activity of the cell cycle-regulating CDK4/6 kinases, Oncogene 38 (30) (2019) 5905–5920.
[16] M.L. Taddei, E. Giannoni, G. Comito, P. Chiarugi, Microenvironment and tumor cell plasticity: An easy way out, Cancer Lett. 341 (1) (2013) 80–96.
[17] N. Schiering, S. Knapp, M. Marconi, M.M. Flocco, J. Cui, R. Perego, L. Rusconi, C. Cristiani, Crystal structure of the tyrosine kinase domain of the hepatocyte growth factor receptor c-Met and its complex with the microbial alkaloid K-252a, Proc. Natl. Acad. Sci. U. S. A. 100 (22) (2003) 12654–12659.
[18] E. Beurel, S.F. Grieco, R.S. Jope, Glycogen synthase kinase-3 (GSK3): Regulation, actions, and diseases, Pharmacol. Ther. 148 (2015) 114–131.
[19] J. Yang, J.i. Nie, X. Ma, Y. Wei, Y. Peng, X. Wei, Targeting PI3K in cancer: mechanisms and advances in clinical trials, Mol. Cancer 18 (1) (2019), https://doi.org/10.1186/s12943-019-0954-x.
[20] W. Wang, L.J. Medeiros, Utility of Cyclin D1 in the Diagnostic Workup of Hematopoietic Neoplasms: What Can Cyclin D1 Do for Us? Adv. Anat. Pathol. 26 (5) (2019) 281–291.
[21] Y.B. Xie, X.F. Shi, K. Sheng, G.X. Han, W.Q. Li, Q.Q. Zhao, B.L. Jiang, J.M. Feng, J. P. Li, Y.H. Gu, PI3K/Akt signaling transduction pathway, erythropoiesis and glycolysis in hypoxia, Mol. Med. Rep. 19 (2) (2019) 783–791.
[22] J.C.H. Cheng, C.H. Chou, M.L. Kuo, C.Y. Hsieh, Radiation-enhanced hepatocellular carcinoma cell invasion with MMP-9 expression through PI3K/Akt/NF-kappa B signal transduction pathway, Oncogene 25 (53) (2006) 7009–7018.
[23] J.-H. Ma, L.i. Qin, X. Li, Role of STAT3 signaling pathway in breast cancer, Cell Commun, Signal. 18 (1) (2020), https://doi.org/10.1186/s12964-020-0527-z10.21203/rs.3.rs-99171/v1.
[24] R.R. Padala, R. Karnawat, S.B. Viswanathan, A.V. Thakkar, A.B. Das, Cancerous perturbations within the ERK, PI3K/Akt, and Wnt/beta-catenin signaling network constitutively activate inter-pathway positive feedback loops, Mol. Biosyst. 13 (5) (2017) 830–840.
[25] N. Awasthi, D. Kronenberger, A. Stefaniak, M.S. Hassan, U. von Holzen, M. A. Schwarz, R.E. Schwarz, Dual inhibition of the PI3K and MAPK pathways enhances nab-paclitaxel/gemcitabine chemotherapy response in preclinical models of pancreatic cancer, Cancer Lett. 459 (2019) 41–49.
[26] Y. Zhang, M. Xia, K.e. Jin, S. Wang, H. Wei, C. Fan, Y. Wu, X. Li, X. Li, G. Li, Z. Zeng, W. Xiong, Function of the c-Met receptor tyrosine kinase in carcinogenesis and associated therapeutic opportunities, Mol. Cancer 17 (1) (2018), https://doi.org/10.1186/s12943-018-0796-y.
[27] F. Moosavi, E. Giovannetti, G.J. Peters, O. Firuzi, Combination of HGF/MET-targeting agents and other therapeutic strategies in cancer, Crit. Rev. Oncol. Hematol. 160 (2021), 103234.
[28] S. Van Schaeybroeck, M. Kalimutho, P.D. Dunne, R. Carson, W. Allen, P.V. Jithesh, K.L. Redmond, T. Sasazuki, S. Shirasawa, J. Blayney, P. Michieli, C. Fenning, H.J. Lenz, M. Lawler, D.B. Longley, P.G. Johnston, ADAM17-Dependent c-MET-STAT3 Signaling Mediates Resistance to MEK Inhibitors in KRAS Mutant Colorectal Cancer, Cell Rep. 7(6) (2014) 1940–1955.
[29] D. Harada, N. Takigawa, K. Kiura, The Role of STAT3 in Non-Small Cell Lung Cancer, Cancers 6 (2) (2014) 708–722.
[30] A. Shen, L.u. Wang, M. Huang, J. Sun, Y.i. Chen, Y.-Y. Shen, X. Yang, X. Wang, J. Ding, M. Geng, c-Myc Alterations Confer Therapeutic Response and Acquired Resistance to c-Met Inhibitors in MET-Addicted Cancers, Cancer Res. 75 (21) (2015) 4548–4559.
[31] M.A. Patil, S.A. Lee, E. Macias, E.T. Lam, C.R. Xu, K.D. Jones, C. Ho, M. Rodriguez-Puebla, X. Chen, Robe of Cyclin D1 as a Mediator of c-Met- and beta-Catenin-Induced Hepatocarcinogenesis, Cancer Res. 69 (1) (2009) 253–261.
[32] C.-G. Huh, V.M. Factor, A. Sanchez, K. Uchida, E.A. Conner, S.S. Thorgeirsson, Hepatocyte growth factor/c-met signaling pathway is required for efficient liver regeneration and repair, Proc. Natl. Acad. Sci. U. S. A. 101 (13) (2004) 4477–4482.
[33] J. Chmielowiec, M. Borowiak, M. Morkel, T. Stradal, B. Munz, S. Werner, J. Wehland, C. Birchmeier, W. Birchmeier, c-Met is essential for wound healing in the skin, J. Cell Biol. 177 (1) (2007) 151–162.
[34] Q.W. Zhang, Z.D. Ye, L. Shi, c-Met kinase inhibitors: an update patent review (2014–2017), Expert Opin. Ther. Pat. 29 (1) (2019) 25–41.
[35] M. Czyz, HGF/c-MET Signaling in Melanocytes and Melanoma, Int. J. Mol. Sci. 19 (12) (2018) 3844, https://doi.org/10.3390/ijms19123844.
[36] J. Li, G. Tan, Y. Cai, R. Liu, X. Xiong, B. Gu, W. He, B. Liu, Q. Ren, J. Wu, B. Chi, H. Zhang, Y. Zhao, Y. Xu, Z. Zou, F. Kang, K. Xu, A novel Apigenin derivative suppresses renal cell carcinoma via directly inhibiting wild-type and mutant MET, Biochem. Pharmacol. 190 (2021), 114620.
[37] G. Pasquini, G. Giaccone, C-MET inhibitors for advanced non-small cell lung cancer, Expert Opin. Investig. Drugs 27 (4) (2018) 363–375.
[38] O. Miranda, M. Farooqui, J. Siegfried, Status of Agents Targeting the HGF/c-Met Axis in Lung Cancer, Cancers 10 (9) (2018) 280, https://doi.org/10.3390/cancers10090280.
[39] J.Y. Wang, Z. Wang, M.Y. Li, Z.H. Zhang, C.L. Mi, H.X. Zuo, Y. Xing, Y.L. Wu, L. H. Lian, G.H. Xu, L.X. Piao, J. Ma, X.J. Jin, Dictamnine promotes apoptosis and inhibits epithelial-mesenchymal transition, migration, invasion and proliferation by downregulating the HIF-1 alpha and Slug signaling pathways, Chem. Biol. Interact. 296 (2018) 134–144.
[40] G.T. Gibney, S.A. Aziz, R.L. Camp, P. Conrad, B.E. Schwartz, C.R. Chen, W.K. Kelly, H.M. Kluger, c-Met is a prognostic marker and potential therapeutic target in clear cell renal cell carcinoma, Ann. Oncol. 24 (2) (2013) 343–349.
[41] J. Peng, S. Qi, P. Wang, W. Li, C. Liu, F. Li, Diagnosis and Prognostic Significance of c-Met in Cervical Cancer: A Meta-Analysis, Dis. Markers 2016 (2016) 1–9.
[42] P. Zhang, S. Li, C. Lv, J. Si, Y. Xiong, L. Ding, Y. Ma, Y. Yang, BPI-9016M, a c-Met inhibitor, suppresses tumor cell growth, migration and invasion of lung adenocarcinoma via miR203-DKK1, Theranostics 8 (21) (2018) 5890–5902.
[43] W. Wang, Q.i. Li, S. Takeuchi, T. Yamada, H. Koizumi, T. Nakamura, K. Matsumoto, N. Mukaida, Y. Nishioka, S. Sone, T. Nakagawa, T. Uenaka, S. Yano, Met Kinase Inhibitor E7050 Reverses Three Different Mechanisms of Hepatocyte Growth Factor-Induced Tyrosine Kinase Inhibitor Resistance in EGFR Mutant Lung Cancer, Clinical Cancer Res. 18 (6) (2012) 1663–1671.
[44] Y.W. Zhang, L.M. Wang, R. Jove, G.F., Vande Woude, Requirement of Stat3 signaling for HGF/SF-Met mediated tumorigenesis, Oncogene 21 (2) (2002) 217–226.
[45] P. Chanvorachote, N. Sriratanasak, N. Nonpanya, C-myc Contributes to Malignancy of Lung Cancer: A Potential Anticancer Drug Target, Anticancer Res. 40 (2) (2020) 609–618.
[46] M. Shtutman, J. Zhurinsky, I. Simcha, C. Albanese, M. D'Amico, R. Pestell, A. Ben-Ze'ev, The cyclin D1 gene is a target of the beta-catenin/LEF-1 pathway, Proc. Natl. Acad. Sci. U. S. A. 96 (10) (1999) 5522–5527.
[47] Tong-Chuan He, Andrew B. Sparks, Carlo Rago, Heiko Hermeking, Leigh Zawel, Luis T. da Costa, Patrice J. Morin, Bert Vogelstein, Kenneth W. Kinzler,

Identification of c-MYC as a target of the APC pathway, Science 281 (5382) (1998) 1509–1512.
[48] Jurriaan B. Tuynman, Louis Vermeulen, Elles M. Boon, Kristel Kemper, Aeilko H. Zwinderman, Maikel P. Peppelenbosch, Dirk J. Richel, Cyclooxygenase-2 inhibition inhibits c-Met kinase activity and wnt activity in colon cancer, Cancer Res. 68 (4) (2008) 1213–1220.
[49] J.D. Holland, B. Gyorffy, R. Vogel, K. Eckert, G. Valenti, L. Fang, P. Lohneis, S. Elezkurtaj, U. Ziebold, W. Birchmeier, Combined Wnt/beta-Catenin, Met, and CXCL12/CXCR4 Signals Characterize Basal Breast Cancer and Predict Disease Outcome, Cell Rep. 5 (5) (2013) 1214–1227.
[50] S. Previdi, P. Maroni, E. Matteucci, M. Broggini, P. Bendinelli, M.A. Desiderio, Interaction between human-breast cancer metastasis and bone microenvironment through activated hepatocyte growth factor/Met and beta-catenin/Wnt pathways, Eur. J. Cancer 46 (9) (2010) 1679–1691.
[51] E.J. McManus, K. Sakamoto, L.J. Armit, L. Ronaldson, N. Shpiro, R. Marquez, D. R. Alessi, Role that phosphorylation of GSK3 plays in insulin, Embo J. 24 (8) (2005) 1571–1583.
[52] V.S.W. Li, S.S. Ng, P.J. Boersema, T.Y. Low, W.R. Karthaus, J.P. Gerlach, S. Mohammed, A.J.R. Heck, M.M. Maurice, T. Mahmoudi, H. Clevers, Wnt Signaling through Inhibition of beta-Catenin Degradation in an Intact Axin1 Complex, Cell 149 (6) (2012) 1245–1256.
[53] B.S. Matada, R. Pattanashettar, N.G. Yernale, A comprehensive review on the biological interest of quinoline and its derivatives, Bioorg. Med. Chem. 32 (2021), 115973.
[54] Annamaria Martorana, Gabriele La Monica, Antonino Lauria, Quinoline-Based Molecules Targeting c-Met, EGF, and VEGF Receptors and the Proteins Involved in Related Carcinogenic Pathways, Molecules 25 (18) (2020) 4279, https://doi.org/10.3390/molecules25184279.
[55] J. Zhang, A. Babic, Regulation of the MET oncogene: molecular mechanisms, Carcinogenesis 37 (4) (2016) 345–355.